The Modified Pressure Bulb Theory Considering Boundary Effect

By

Ahmed Raji

A thesis submitted to
the Faculty of Graduate Studies
in partial fulfilment of
the requirements for the degree of
Master of Science

Department of Mechanical Engineering
Faculty of Graduate Studies
University of Manitoba
Winnipeg, Manitoba

May 2024

Abstract

This study investigates the behavior between Finite Element Analysis (FEA) results and the modified Westergaard equation, taking into consideration of the boundary effect on stress distribution around the loading area of a mechanical part with limited dimension. The Westergaard equation, a definitive problem-solving method in elasticity of pavement with 'boundary at infinity approximation', serves as the theoretical basis while a modified advancement is introduced to optimize parameters and address differences between theoretical assumptions and FEA results. The study emphatically included boundary effects in the analysis, acknowledging their effect on stress patterns.

Parameters, such as stress measurement horizontal location (r) and stress measurement depth (Z), are systematically modified, and a new variable, load-to-boundary distance (LB), is introduced to achieve a more accurate alignment between FEA and the newly tuned Westergaard theoretical results. This finding noted the relevance of the original Westgaard model error as well as the boundary effect in tuning the original Westergaard equation, contributing to real-life engineering applications, especially on mechanical parts with limited dimensions. More specifically, the original Westergaard model is tuned by introducing polynomial constants (A and B factors) to correct its error in the application of mechanical parts with a single material. The boundary effects of mechanical structure with limited dimensions and its induced stress distribution error can be described by a Gaussian function with variable, LB.

Acknowledgement

I would like to express my sincere gratitude to everyone who has contributed to the completion of this thesis. First and foremost, I am deeply thankful to my advisor Dr. Nan Wu for his unwavering support, guidance, and invaluable insights throughout the research process. His mentorship has been instrumental in shaping the trajectory of this work.

I express my gratitude to Dr. Larry Liang and Dr. Yuejian Chen, who served as members of my thesis committee, for their invaluable time, perceptive feedback, and critical assessments. Their scholarly and practical contributions have enhanced my research and expanded its scope. Their advice and criticism have been helpful in helping me polish my ideas and raise the overall standard of this thesis.

I also express my heartfelt gratitude to my wife and daughter who had been shown me great support throughout the course of this journey. They created an enabling and conducive environment for me to excel on this course, I am incredibly grateful for the love and moral support.

Finally, I express my gratitude and thanks to my family and friends for their understanding and encouragement. Their support inspired me to overcome challenges and remain firm.

Contents

List of Symbols

K (r, LB): *Tuning function considering the boundary and edge effect*

r: Radial Distance between the loading point and measurement point

Z: Depth of the measurement location

A(r)*: Multiplying constant function to directly influences the amplitude of the stress distribution curve around the loaded region.*

B(r)*: Multiplying constant function specifically to adjusts the curvature of the stress distribution function.*

n (μ): *Poisson's ratio function*

LB: Loading Boundary Distance

$\sigma z_n(r, Z)$: *Stress function at any location*

μ*: Poisson's ratio*

ZK (Z, LB): *Depth effect corrections factor on K(r, LB)*

ZA(Z*): Depth effect corrections factor on A(r)*

ZB(Z): *Depth effect corrections factor on B(r)*

FEA: Finite Element Analysis

Chapter 1 Introduction

Stress analysis plays a critical role in engineering materials and structures, as it allows engineers to predict how components will behave under various loads, ensuring their safety and longevity. Understanding the distribution of stress within materials is vital for designing robust mechanical parts, as poorly designed components can fail under stress, leading to costly repairs or even catastrophic failures.

In engineering, stress analysis is typically conducted using numerical methods, such as Finite Element Analysis (FEA), which provides detailed insights into the stress distribution within complex structures. However, analytical models, like the Pressure Bulb Theory, offer simplified solutions to understand stress distribution patterns in elastic half-spaces under concentrated loads (Gazetas, 1991). These models serve as a foundational tool for engineers, especially in early-stage design (Coduto, Yeung, M. R., & Kitch, W. A., 2001).

The Westergaard model is one such analytical approach, originally developed for concrete slabs subjected to point loads. It offers insights into stress distribution within homogeneous, elastic materials (Westergaard H. M., 1926). While valuable, this model was designed for large, shallow surfaces, and its assumptions limit its accuracy in cases with significant boundary effects or heterogeneous materials (Das B. M., 2007). In mechanical structures, the assumptions of linear elasticity and homogeneity may not be suitable, requiring modifications or advanced numerical techniques to provide accurate predictions (Terzaghi & Peck, R. B, 1943). Thus, detailed stress analysis methods, including FEA are often necessary to complement or replace traditional analytical approaches in modern engineering applications (Bowles, 1996).

1.1 Background

Stress analysis is fundamental in engineering, as it helps predict the behavior of structures and materials under various loading conditions. Numerical methods such as FEA are widely employed to analyze stress distributions in complex systems (Burmister, 1945). On the other hand, analytical models like the Pressure Bulb Theories including the Westergaard's equation offer simplified approaches to estimate stress distribution under certain conditions. Westergaard's equation, initially developed for analyzing stress in concrete slabs and pavement layers has been adopted in this study for mechanical structures. However, when applied to mechanical parts, the primary distinction lies in the material properties, such as Young's modulus and Poisson's ratio, which differ from those of concrete, leading to variations in stress intensity and distribution (Westergaard H. M., 1938).

The Westergaard model, developed in the early 20th century, is foundational for evaluating stress in homogenous, elastic half-spaced structure under loading (Westergaard H. M., 1926). Its limitations, such as assumptions of linearity, homogeneity, and isotropy, can reduce its accuracy when applied to real-world structures, which often exhibit nonlinear and anisotropic behaviors (Coduto, Yeung, M. R., & Kitch, W. A., 2001).

For structures, the Westergaard model works best in cases where the depth of the loaded area is small compared to the overall dimensions of the part (Terzaghi & Peck, R. B, 1943). In situations involving larger depths or complex material interactions, the model may fail to accurately predict stress distribution (Bowles, 1996). These limitations highlight the need for advanced numerical methods, such as FEA, particularly in mechanical engineering applications where accurate stress predictions are critical for ensuring structural integrity (Gazetas, 1991).

1.2 Literature Review

In this study, exploring the advancements in stress analysis methods and their applications in mechanical engineering, starting with general stress distribution techniques and concluding with specific pressure bulb models will be done. The field has evolved from traditional analytical methods to modern numerical approaches, offering better solutions to complex engineering problems. The review will first introduce key developments in computational techniques and theoretical frameworks, followed by a detailed discussion of pressure bulb theories and their adaptation to mechanical structures.

Stress analysis plays a crucial role in understanding how mechanical structures behave under load. As mechanical engineering continues to advance, methods like FEA and other numerical modelling techniques have become indispensable in predicting the stress distribution within materials, especially for complex geometries, variable boundary conditions, and diverse material properties. These techniques have enabled engineers to move beyond the limitations of early analytical methods by offering highly precise and adaptable tools for evaluating stress and strain in real-world applications. Modern structural analysis methods also incorporate probabilistic frameworks to address uncertainties in boundary conditions, further enhancing reliability and performance predictions.

1.2.1 Recent Advances

The development of an approach that involved modeling the structure as a thin, indefinite, or semi-infinite plate resting on a bed of springs to calculate the reaction of stiff components subjected to loads. This method allows for the analysis of stress distribution and deformation in structures, particularly those under heavy or repeated loading conditions (Westergaard H. M., 1926).

In recent years, the field of stress analysis in structural engineering has witnessed significant advancements, particularly with the development of more sophisticated numerical methods and analytical solutions. Modern computational techniques, such as FEA, have become invaluable tools for engineers to model and simulate complex stress patterns in materials and structures. These methods allow for the precise analysis of stress distributions under various loading conditions, accounting for factors such as material heterogeneity and non-linear behavior, which were difficult to address with earlier theories.

Alongside numerical approaches, there have been developments in probabilistic frameworks that incorporate uncertainties in boundary conditions and material properties, helping to improve the reliability of stress predictions in real-world applications. Analytical solutions, while often constrained by idealized assumptions, continue to play a role in offering insights into foundational concepts of stress behavior. The Westergaard model, for example, remains one of the key analytical methods for studying stress distributions, though it will be introduced in more detail in a later section.

These advancements reflect the ongoing evolution of both traditional theories and modern computational tools, enabling more accurate and adaptable approaches to stress analysis in structural engineering.

1.2.2 Introduction of Computational Techniques for Stress Analysis

In structural engineering, computational techniques such as FEA and other numerical methods have become essential tools for accurately predicting and analyzing stress distribution in complex structures. These techniques are designed to overcome the limitations of traditional analytical models, which often rely on idealized assumptions and may fail to capture the full range of real-world variables such as material nonlinearity, boundary conditions, and complex

geometries. By leveraging these computational tools, engineers can simulate stress behaviors under various loading conditions, improving the reliability of structural design and analysis.

Emphasizes on investigation of how difficult it is to take the closeness of boundaries into consideration while analysing the stress. The findings showed that taking into consideration the effect of boundaries close-by might critically change the distribution of stresses anticipated by pressure bulb theory (Burmister, 1945). Contribution was made to support these outcomes even more by emphasizing on the changes needed to correctly predict stress in constrained geometries (Bell, 1954).

Investigating stress distribution in structures has improved greatly with the incorporation of computer tool, mostly FEA. Using FEA to check structure interactions, scholars were able to get in-depth understanding of stress distribution. Their study exposed flaws in conventional Pressure Bulb Theories and pointed the need of considering boundaries effect on structures (Randolph, Wroth, C. P., & Farmer, I. W., 1982) (Potts & Addenbrooke, T. I., 1991).

To resolve the issues of these restrictions, new advancements in numerical methods, particularly FEA, have gained attention. A more in-depth study of stress patterns is made possible by FEA, which take into considerations varied materials, and complicated geometries. Scholars have made important contributions to the advancement and use of FEA in structural study, providing an important tool for precisely investigating stress distribution (Bathe K. J., 2006)(Zienkiewicz, O. C & Taylor, R. L, 2000)

1.2.2.1 Numerical Methods

The FEA methods became a complement to the Westergaard equation as the computation methods advanced. Westergaard's analytical method was validated and supported FEA of structures (Clough, Wilson, E. L, & Paris, P. C, 1960), which showed the impact of the numerical solutions in capturing more complex stress distribution.

Engineering uses numerical techniques, especially FEA, extensively to model and investigate the distribution of stress in solids. In FEA, a structure is discretized into a finite number of elements, and the stress-strain equations for each element are solved. This approach is especially helpful for engineering design and optimisation as it enables thorough modelling of intricate geometries and material behaviours. FEA produces extremely precise results for stress distribution in complicated structures, and it can handle a broad range of loading circumstances and limitations. FEA is a typical tool in areas including automotive, aerospace, and civil engineering because of its adaptability (Zienkiewicz, O. C & Taylor, R. L, 2000) (Reddy, 2006).

Pros and cons of Numerical Method

- High accuracy for complex geometries and loading conditions.
- Ability to model a wide range of material behaviors.
- Versatility in handling various constraints and boundary conditions.
- Useful for design optimization and failure analysis.
- Requires significant computational resources.
- Time-consuming for very large or complex models.
- Results can be sensitive to the quality of the mesh and element type.
- Requires expertise in both the software and the underlying mechanics.

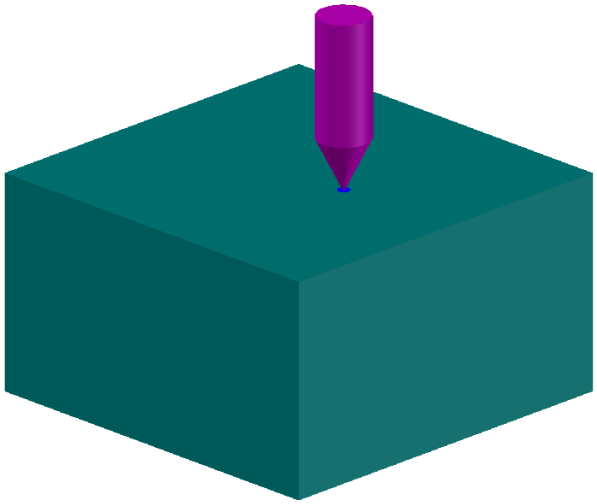

Figure 1- 1: FEA on a structure.

1.2.2.2 Theoretical and Analytical Methods

Equations based on the fundamentals of mechanics and material science are derived in theoretical ways. These techniques depict the distribution of stresses in a material under different loading scenarios using mathematical models. For instance, the connection between stress and strain in elastic materials is described by equations found in the theory of elasticity (Timoshenko & Goodier, J. N, 1951). The development of analytical solutions for simpler geometries and loading circumstances, as well as the comprehension of the fundamental concepts underpinning stress distribution, depend heavily on theoretical approaches. They support the validation of numerical models and serve as the basis for more intricate numerical studies.

Pros and Cons of Theoretical Methods

- Provides fundamental understanding of stress distribution.
- Essential for deriving analytical solutions.
- Useful for validating numerical models and simulations.

- Generally, less resource-intensive than numerical methods.
- Limited to simpler geometries and boundary conditions.
- Assumptions may not always reflect real-world conditions.
- Can be mathematically intensive and complex to derive solutions.

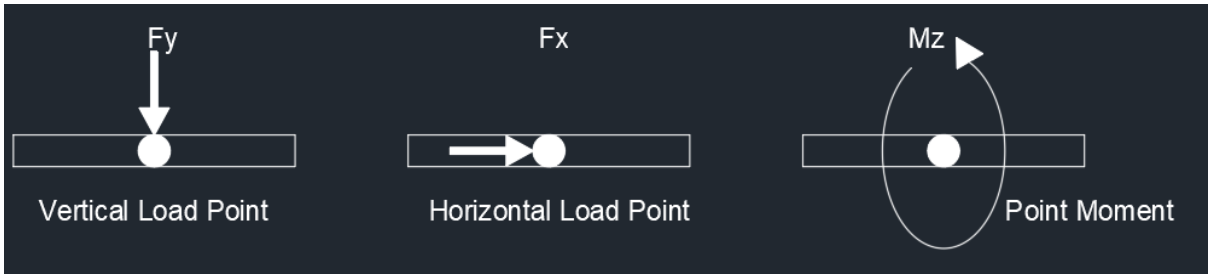

Figure 1- 2: Theoretical method analysing applied load on a structure.

There are several sorts of theoretical approaches available for analysing stress distribution in solids, each with unique uses and underlying assumptions. These techniques lay the groundwork for more intricate numerical studies and are crucial for obtaining analytical solutions to solid mechanics issues. The primary kinds of theoretical approaches are as follows:

I. Elastic Theory

The behaviour of solid materials that deform when external forces are applied but return to their original shape when those forces are removed is the subject of the theory of elasticity. Hooke's Law, which describes the linear connection between stress and strain, is the foundation of this theory. The compatibility criteria for strain and the Navier-Cauchy equations are important formulas in elasticity theory. Stress and strain issues in materials subjected to different kinds of loading, such as tension, compression, bending, and torsion, are resolved using the theory of elasticity (Timoshenko & Goodier, J. N, 1951).

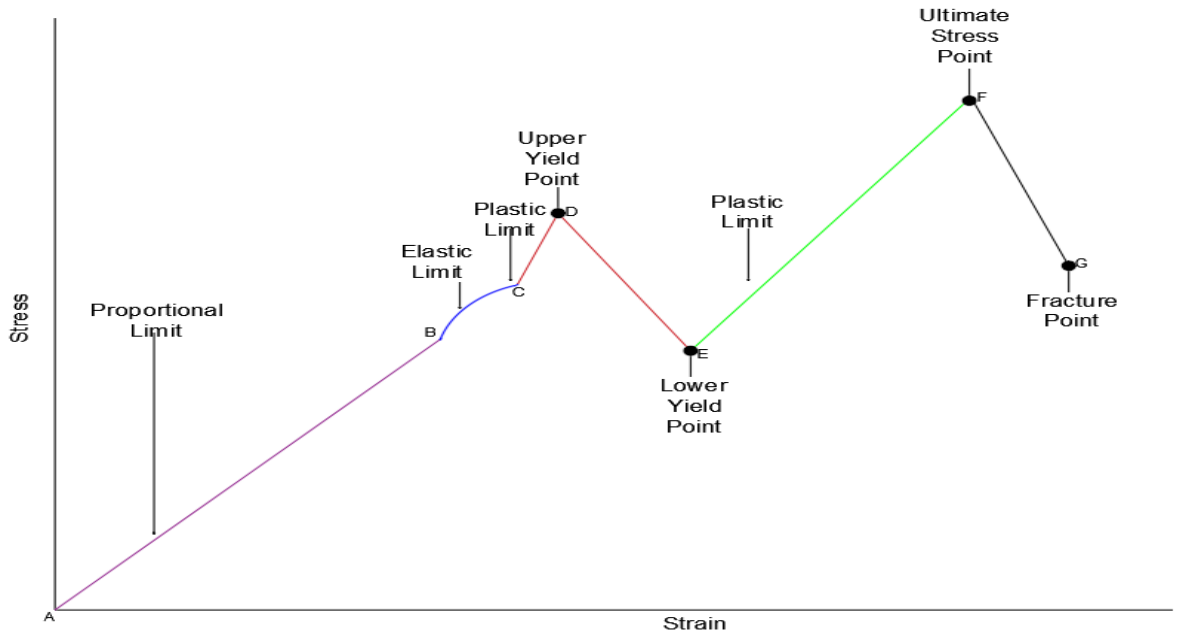

Figure 1- 3: Stress-Strain curves showing different region during loading of a mechanical structure.

II. Plastic Theory

The behaviour of materials that experience persistent deformation when stressed beyond their elastic limit is explained by the plasticity hypothesis. Understanding and forecasting how materials like metals and polymers will behave under high-stress circumstances depends heavily on this theory. Hardening rules, flow rules, and yield criteria (such as the von Mises and Tresca criteria) are important ideas in plasticity. The theory of plasticity has extensive application in domains including materials science, structural engineering, and metal forming.

III. Fracture Mechanics

The study of material cracks and the circumstances under which they spread and eventually result in failure is the focus of fracture mechanics. This discipline analyses the stress and strain fields close to fracture tips by combining concepts from plasticity and elasticity. Stress intensity parameters, energy release rates, and fracture toughness are important ideas. For the purpose of creating materials with increased resistance to cracking and for forecasting the failure of

structures and materials under diverse loading circumstances, fracture mechanics is crucial (Anderson, 2017).

IV. Viscoelasticity Theory

According to viscoelasticity theory, materials that undergo deformation can behave in both an elastic and viscous manner. These materials exhibit time-dependent stress-strain relationships, including biological tissues and polymers. Elasticity and viscosity are combined in viscoelastic models, including the Maxwell and Kelvin-Voigt models, to describe the behaviour of the material. This hypothesis is especially significant for analysing materials that undergo creep and long-term stress.

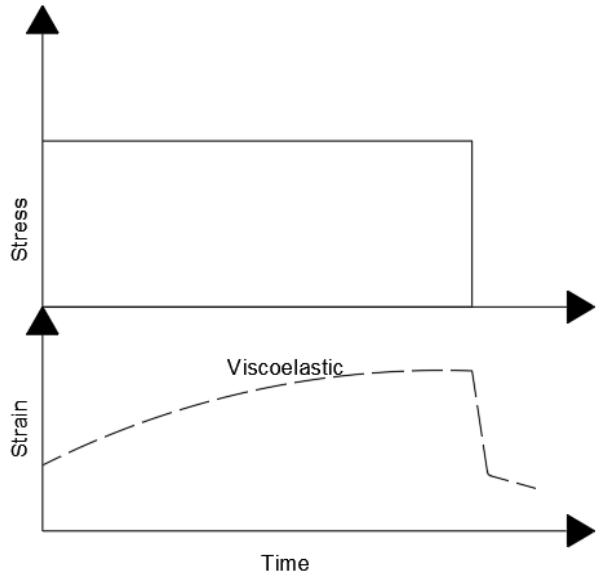

Figure 1- 4: Viscoelasticity in structure.

V. Thermoelectricity

Thermoelectricity theory examines how mechanical and thermal fields interact with solid materials. It examines how temperature variations impact stress and strain distributions by fusing the ideas of thermodynamics and elasticity. Heat conduction equations and coefficients of thermal expansion are included in thermoelastic equations. In the fields of mechanical,

aeronautical, and civil engineering, where thermal effects play a major role, this theory is crucial for finding solutions.

VI. Hyperelasticity

The nonlinear elastic behaviour of materials, especially rubber-like compounds and biological tissues is referred to as hyperelasticity or green elasticity. Hyperelastic materials, in contrast to linear elasticity, can experience significant deformations before recovering to their original shape when loaded. The stress-strain behaviour of these materials is characterised by hyperelastic models, such as the Neo-Hookean and Mooney-Rivlin models. In biomechanics and the design of flexible components and structures, this idea is essential (Ogden, 1997).

The basic instruments for comprehending and forecasting the behaviour of materials under varied loading scenarios are provided by these theoretical approaches. They provide the foundation for more intricate numerical models and simulations, guaranteeing the efficiency and safety of engineering projects.

Analytical techniques solve the governing equations of mechanics directly, yielding closed-form solutions to stress distribution issues. Usually, these techniques work with simpler geometries and boundary conditions where the equations have accurate solutions. The stress analysis of beams, plates, and shells under various loading scenarios are classical examples. In addition to being excellent resources for understanding how materials and structures behave, analytical techniques can act as standards for certifying numerical simulations (Timoshenko & Goodier, J. N, 1951). Analytical solutions provide accurate and timely evaluations of stress distribution in idealised circumstances, notwithstanding their limits in addressing complicated geometries.

Pros and Cons of Analytical Methods

- Provides exact solutions for simple problems.
- Quick and efficient for idealized scenarios.

- Useful as benchmarks for numerical methods.
- Offers clear insights into the behavior of structures.
- Limited to simple geometries and boundary conditions.
- Not applicable to complex real-world problems.
- Solutions can be difficult to obtain for non-standard conditions.

Combining these methods often provides the most robust analysis. For instance, theoretical and analytical methods can be used to understand and validate the results obtained from numerical simulations like FEA. Each method's strengths complement the others, offering a comprehensive approach to studying stress distribution in solids. The choice of method depends on the problem's complexity, the required accuracy, and the available computational resources.

1.2.3 Pressure Bulb Models

Pressure bulb theories are critical in the analysis of stress distribution within mechanical components subjected to point or distributed loads. Originally applied in geotechnical engineering, these models have been adapted for use in mechanical structures to provide insight into how applied forces propagate through materials such as metals and composites. These theories enable engineers to visualize how stresses from external loads are distributed internally, particularly in regions around the point of load application.

For mechanical parts, the pressure bulb concept helps determine the depth and extent of stress penetration within a component. This is vital for identifying zones of stress concentration, which can be critical for predicting failure points or regions that may require reinforcement. Whether dealing with machine components, metal structures, or mechanical systems,

understanding how stress distributes through the material is essential for ensuring that parts can withstand operational loads without excessive deformation or failure.

These theories are now integral in mechanical design and analysis, providing engineers with the tools needed to optimize part strength and durability. Understanding the stress distribution via pressure bulb theories is crucial for ensuring that mechanical components perform reliably under load, especially in critical applications where stress concentrations can lead to fatigue or failure.

1.2.3.1 Concept of Pressure Bulbs

Pressure bulb models depict zones of equal stress, known as isobars, within the soil or rock mass. These isobars form concentric, bulb-shaped regions, indicating the intensity and distribution of stress at various depths and distances from the load. This visualization helps engineers determine the depth and extent of stress influence, essential for assessing soil bearing capacity, settlement, and potential shear failure (Das B. , 2010). The types of pressure bulb theory include the following models.

I. Boussinesq Pressure Bulb Model

Developed by Joseph Valentin Boussinesq, this model applies to a point load on the surface of a semi-infinite, homogeneous, isotropic, elastic half-space (Boussinesq, 1885). It is widely used for analyzing stress distribution under footings and other surface loads. The pressure bulbs are symmetrical about the vertical axis and extend deeper as the distance from the load increases.

II. Newmark's Influence Chart

A graphical method used to determine stress distribution under a uniformly loaded area (Newmark, 1942).The chart allows for the superposition of stress increments from different parts of the loaded area to obtain the total stress at any point beneath the loaded area.

III. Westergaard Pressure Bulb Model

The Westergaard model, originally developed in 1938, was designed to account for the rigidity of materials and provide solutions for stress distribution beneath rigid foundations (Westergaard H. M., 1938). While initially applied in geotechnical engineering for analysing stresses under point loads in rigid foundations, its underlying principles offer potential for broader applications, particularly in mechanical structures. One of the model's strengths is its ability to handle stratified materials, such as soils or layered structures, where stiffness properties vary between layers. However, in the context of mechanical systems, additional factors like boundary effects and material heterogeneity play crucial roles in stress distribution.

This research focuses on the Modified Pressure Bulb Theory Considering Boundary Effect in mechanical structures, and the Westergaard model was selected for its consideration of Poisson’s ratio effect in the Westgaard model making it more robust dealing with stress distribution in different materials and applications. Furthermore, the Westgaard model was invented and applied to simulate the stress in layered materials, and the different layers edge effects were evaluated in the model making it potentially more suitable to consider the boundary effect on stress distribution in structures with limited dimension. However, the original Westergaard model assumes isotropic materials with continuum boundary conditions that may not align with the complex, real-world behaviour of mechanical parts. For this reason, the model needed to be tuned to account for the open or discontinued boundary conditions.

By modifying the Westergaard model to incorporate boundary effects, this study aims to enhance its precision for predicting stress distributions in mechanical structures. This tuning process allows the model to better reflect the complex interactions between material properties and structural boundaries, which are critical factors in modern mechanical engineering. Ultimately, the goal of this research is to demonstrate that by adapting the Westergaard model, its applicability can be expanded to more complex mechanical environments, improving its reliability in cases where traditional models fall short.

1.2.3.2 Applications of Pressure Bulb Models

The pressure bulb theory, originally developed in geotechnical engineering for understanding stress distribution in soils and pavement layers under loads, has inspired similar concepts in mechanical engineering. While its primary application has been in analysing stress distribution beneath foundations and in layered pavement structures, the underlying principles of stress propagation have found relevance in the study of mechanical components. In pavement engineering, the theory is particularly useful for assessing how composite materials like asphalt and concrete respond to applied loads. In mechanical engineering, although the theory is not directly used, its concepts are adapted to understand how stress distributes within mechanical parts under point or distributed loads. These adaptations help engineers assess potential zones of stress concentration and evaluate material behaviour in structural components. However, more advanced computational techniques like FEA are often preferred for complex mechanical systems due to their ability to model intricate geometries and material properties more accurately. The Westergaard model is based on a mathematical framework that provides detailed analytical solutions for stress distribution in elastic materials under point loads. Its structure allows for the calculation of stress not just directly beneath the load but also across varying depths and radial distances. This makes the model highly useful for understanding how stress propagates away from the point of load, particularly toward the edges of a structure.

In stress analysis near the edge of mechanical parts, boundary conditions have a significant impact on how stresses are distributed. Many simpler models, such as Boussinesq's one, assume an infinite, homogenous medium, where boundary effects are ignored. However, in real-world mechanical parts, especially when the part has finite dimensions, the proximity of edges alters the stress field dramatically. Stress concentrations tend to build up near edges or corners, especially where loads are applied close to the boundary.

The framework of the Westergaard model accounts for the rigidity of materials with different Poison's ratios and can be adapted to include the effects of nearby boundaries, making it well-suited for edge analysis. Unlike simpler models, the Westergaard approach can be modified to consider variations in material stiffness or constraints caused by edges or interfaces between different materials. This flexibility is one of the key reasons why it can be tuned for mechanical structures, where edge effects must be accurately modeled to predict stress concentrations.

In summary, the Westergaard model's analytical framework provides a detailed understanding of stress distribution across both central and boundary regions, making it adaptable for analyzing stress near the edges of mechanical structures where boundary effects are critical.

Below are some key applications:

I. Stress Analysis in Machine Components:

With further tuning, the pressure bulb theory could be applied to study stress propagation within machine components under external loads. This adaptation would be particularly valuable for analysing stress distribution around features such as holes, notches, or other discontinuities in mechanical parts like gears, shafts, or bolted joints.

II. Design of Pressure Vessels:

In the context of pressure vessel design, an optimized pressure bulb theory could help predict how internal pressures distribute stresses throughout the vessel material. This application would be crucial for ensuring that pressure vessels can withstand operational pressures without failure, enhancing structural integrity in containment structures.

III. Fatigue and Fracture Mechanics:

The theory assists in identifying zones within mechanical components that are prone to high-stress concentrations, which are critical areas for initiating fatigue cracks or fractures. By understanding the stress distribution, engineers can enhance the durability of components by redesigning or reinforcing critical areas.

IV. Foundation and Support Structures:

For mechanical systems that require support structures, such as heavy machinery or equipment mounted on platforms, the pressure bulb theory helps in designing the foundations. It predicts how the load from the machinery distributes through the support structure and into the ground, ensuring stability and preventing excessive settlement.

V. Stress Analysis in Welded Joints:

With suitable tuning, the pressure bulb theory could be adapted to analyze stress distribution around welds in welded structures, especially in areas with significant geometric or material changes. Such an application would be essential for preventing weld failures and ensuring the integrity of welded joints under load, contributing to overall structural reliability.

VI. Optimization of Load-Bearing Components:

The theory can be used to optimize the design of load-bearing components by predicting stress distribution and identifying areas that may require additional material or reinforcement. This

leads to more efficient use of materials and enhances the performance of the component under load.

1.2.3.3. Advantages and Limitations

While this Pressure Bulb Model provides valuable insights into stress distribution and helps in optimizing design by identifying stress concentrations, it also comes with limitations. These include assumptions about material properties and boundary conditions that may not always align with real-world scenarios. Understanding both the strengths and constraints of this theory is essential for its effective application in the analysis of mechanical parts under load.

I. Advantages:

- Adaptation to Complex Geometries: The pressure bulb theory, when applied to mechanical parts, can be adapted to analyze complex geometries and load conditions, making it versatile in assessing stress distribution in various mechanical components.
- Identification of Stress Concentrations: Just as in civil engineering, the theory helps in identifying zones of stress concentration in mechanical parts, which are critical for fatigue analysis and failure prevention, ensuring the durability and safety of the components.
- Optimization of Design: By understanding stress distribution within a mechanical part, engineers can optimize the design to minimize stress concentrations, leading to more efficient and reliable components.
- Support for Material Selection: The theory can guide the selection of materials by predicting how different materials will behave under load, ensuring that the mechanical part will perform as intended under operational conditions.

II. Limitations:

- Assumptions on Material Properties: The theory assumes homogeneous and isotropic material properties, which may not hold true for composite materials or advanced alloys commonly used in mechanical parts. This could lead to inaccurate predictions of stress distribution.
- Simplification of Complex Mechanical Behavior: In mechanical engineering applications, components often experience complex loadings, including dynamic, thermal, and multi-axial stresses, which may not be fully captured by the pressure bulb theory.
- Neglect of Microstructural Effects: Mechanical parts often have microstructural features, such as grain boundaries, inclusions, or phase transformations, which can significantly influence stress distribution. The pressure bulb theory may not account for these factors, leading to oversimplified results.
- Boundary Condition Sensitivity: The accuracy of predictions in mechanical parts may be highly sensitive to the assumed boundary conditions, which can differ significantly from actual operating conditions, especially in cases involving complex constraints or interactions between components.
- Scale Limitations: The theory is more traditionally used for large-scale applications, such as in geotechnical engineering. When applied to small mechanical parts, the scale differences might introduce errors, as the theory may not adequately capture the localized stress variations in small-scale components.

The pressure bulb theory provides valuable insights into stress distribution for various applications in mechanical engineering. While originally intended for geotechnical applications, its principles have been successfully adapted to improve the design, analysis, and optimization of mechanical components. However, engineers must consider the

theory's limitations and ensure it is applied appropriately within the context of their specific mechanical engineering challenges.

1.2.4 Empirical Insight from Laboratory Experiment

Concurrently, laboratory investigation carried out by researchers gave resourceful information about the importance to consider boundary conditions when working with structure. By thorough experiments, these researchers showed the useful effect of boundary impacts on stress distribution predictions, offering a concrete basis for improving the Modified Pressure Bulb Theory (Viggiani, Atkinson, J. H., & Springman, S. M., 2000) and (De Mello & McCabe, B. A., 1992).

By considering boundary effect in mechanical parts in this study and using the capabilities of modern numerical simulations, the Tuned Pressure Bulb Theory has emerged as an enhancement of original Pressure Bulb Theory in the case of mechanical structure. Recent studies showed a good example of how efforts are being made to take nearby boundaries into consideration to enhance the accuracy of stress calculations under loaded structure

A crucial component of material science and structural engineering is the study of stress distribution in solids, which involves the transmission of forces through solid materials. Stress distribution is analysed and predicted using a variety of techniques, including analytical, theoretical, and numerical techniques like FEA. Depending on the required accuracy and problem complexity, each solution has pros and cons of its own.

1.2.5 Summary of Challenges and Limitations

In the case of mechanical structures, the tuned pressure bulb theory, especially when considering boundary effects, represents an advancement in understanding stress distribution directly under loading points. The conventional pressure bulb theory which was initially

considered by Westergaard in the early 20th century, has been a critical tool for calculating stresses induced by concentrated loads on elastic half-spaces. However, as engineering applications advances, it became evident that the original Westergaard equation did not adequately capture the complexities brought by Poisson ratio and boundary conditions in structures.

The current research gaps lie in the limitations of traditional stress distribution models, such as the classic Westergaard and Boussinesq theories, did not consider mechanical parts in stress distribution analysis. Additionally, when used on mechanical parts, the existing models struggle with predicting stress distributions in regions with significant curvature or intricate boundary constraints, making them less reliable for modern engineering applications.

Filling these gaps involves developing an enhanced theoretical framework. By addressing these limitations, engineers can achieve more accurate stress distribution predictions on mechanical parts with limited dimensions, leading to optimized component designs, improved performance, and better failure prevention strategies. Ultimately, closing these gaps will provide more robust tools for analyzing and designing mechanical systems under real-world conditions.

1.3 Objectives

The first key aim of this research is to evaluate whether the existing Westergaard model, originally developed can be directly applied to mechanical parts made from isotropic linear elastic materials. Before considering the boundary effect, it is essential to assess and tune the model to see if it accurately predicts stress distribution for these materials. This involves fine-tuning the Westergaard model to ensure its precision in capturing stress patterns in mechanical structures. Only after confirming the model's applicability will the next step involve modifying

the pressure bulb theory to account for the boundary effects. This two-step approach ensures a solid foundation in stress analysis for isotropic linear elastic mechanical parts, which is critical for reliable structural designs.

The second goal is to study how boundary affects the distribution of stress in mechanical structure. Understanding the effect of boundaries on stress distribution is important for supporting current theories and introducing more precision in models for real-world engineering applications.

Additionally, the validation of theoretical and numerical models versus real-world engineering studies is especially important. The aim of this validation steps is to enhance the models so that they can predict stress distribution under mechanical structure with precision and dependability. Analysis of stress will continue enhanced with the help of the input from real-world applications.

The utmost aim is to combine the results into useful engineering design recommendations. These recommendations will explore the Tuned Pressure Bulb Theory with adjustments to boundary effects, considering relevant resources to improve mechanical structural design and performance prediction.

Specifically speaking, the enhancement of the use of pressure bulb theory in the case of mechanical structures considers the effects of boundary and the theoretical description of the stress distribution in mechanical parts with limited dimensions.

1.5 Thesis Organization

In chapter 2, as a ground truth reference, the FEA model and results are provided by describing FEA and software used, structure dimension, boundary and loading condition, as well as discrepancies between the FEA and Westergaard results. In chapter 3, critical functions that

influence the stress distribution were introduced for study in mechanical structures to fine-tune the Westgaard model and better align the theoretical predictions with the results obtained from FEA. The boundary effect of the part under loading with limited dimension on stress distribution at different measurement locations were included and discussed to derive a general analytical formula describing the stress distribution from a point load. Furthermore, in chapter 4, the validation of the tuned Westergaard model were conducted with different part size and loading conditions. And finally, the conclusions and future works on the newly proposed theoretical model was provided in the chapter 5.

Chapter 2 Finite Element Model and Results

In this chapter, the use of the FEA to accurately model and analyze the stress distribution in a structure with required dimensions will be done. The objective is to make visible the formation of the pressure bulb under the loaded area at different *LB*. Additionally, the exploration of different boundary and loading conditions and their impacts on the structure's behavior will also be illustrated as the ground truth to tune the theoretical model.

2.1 Using FEA for finding the real accurate results of stress distribution in a structure with finite dimension.

To model and analyse the distribution of stresses, deformation, and other physical behaviour of structures with finite dimensions, engineers often utilise the sophisticated numerical method known as FEA (Zienkiewicz & Taylor, 2005). Due to the method's adaptability, structures of any complexity may be modelled, regardless of their intricate geometric design (Bathe K. J., 1996). With the use of FEA, engineers can model structures in great depth and accuracy, considering complicated geometries and irregular shapes.

The fact that FEA can tackle a wide range of materials, including those with nonlinear stress-strain patterns, is one of its main advantages (Cook, Malkus, D. S., & Plesha, M. E., 2001). This specific capability comes in handy when checking constructions composed of materials that behave nonlinearly under various loading situations.

Professionals can examine the effect of various design factor on stress distribution by conducting parametric simulations with FEA (Bathe K. J., 1996). This strategy assures the resilience and effectiveness of a design and is importance for optimization and sensitivity evaluation.

Moreover, fatigue analysis, which assesses how repeated loading over time changes the stress distribution in a structure, may be performed with FEA (Zienkiewicz & Taylor, 2005). This is necessary to evaluate the structural components' long-term integrity and durability.

To assure correctness and dependability, FEA findings maybe checked and confirmed against experimental data (Cook, Malkus, D. S., & Plesha, M. E., 2001). Integrity of numerical forecast is established by calibration using physical testing.

Finally, professionals can easily visualise and analyse stress distribution data because to the comprehensive post-processing capabilities offered by FEA software. This improves understanding of the structural reaction and includes animations, contour graphs, and Von Mises stress calculations (Bathe K. J., 1996).

2.1.1 FEA Method and Software Used in the Study

ANSYS is one the most used software package for doing FEA. A full range of simulation tools, including capacities for fluid dynamics, electromagnetic, thermal, and structural analysis, are included in ANSYS. Professionals that are working on complex simulations often use ANSYS because of its reputation for having a user-friendly interface, strong solver, and strong post - processing tools.

A computational method for resolving engineering problems involving fluid dynamics, heat transfer, structural mechanics, and other physical processes is FEA. The method breaks down complex systems or structures into smaller, easier-to-manage components, checks the behaviour of each component, and then compiles the findings to understand the system's overall reaction. The approach is frequently used for design optimization, simulation, and analysis in many engineering fields.

The first crucial step in the FEA process was modelling of an 18mm x 18mm x 18mm stainless steel structure using ANSYS 2023 Workbench software, considering that noticeable stress is typically distributed within 6mm from the loading point and/or the boundary. All necessary material properties, loading conditions, and boundary constraints were defined according to the problem requirements. Proper meshing, element types, and convergence criteria were employed to ensure accurate results. A specified point load was applied at various loading boundary distances of 9mm, 6mm, 3mm, and 1mm, and the FEA results were subsequently generated.

The condition of the boundary is set up to define how the structure would interact with its environment in the real world. To imitate the situations the structure would encounter in real-world, loads and limits must be applied. The next stage is the solver execution phase, when a system of equations describing how the structure behaves under given situations is solved numerically to get an approximation of the solution.

An important phase in the FEA process is post-processing which entails analysing and interpreting the solver output. Tools for creating graphical presentations, including stress contours and deformation plots, are available in ANSYS and other FEA software systems. These tools give crucial details for additional investigation.

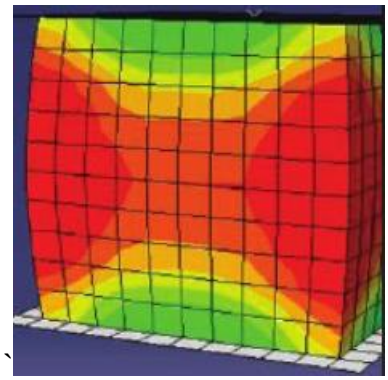

Figure 2- 1: FEA on a Mechanical Structure.

2.1.2 Details of the Structure and Model

A structural steel of 12mm x 12mm x 12mm dimension was being investigated. FEA is used to analyse this model, which was believed to have a basic cuboid shape, and to understand its behavior under different conditions. The cubic structure was selected for this research because of its straightforwardness and practical significance in engineering contexts. Numerous mechanical parts and structural components have rectangular or cubic forms, rendering it a representative geometry for studying stress distribution when subjected to point loads. The cubic configuration facilitates an uncomplicated assessment of boundary effects and stress concentrations, particularly at corners and edges, which are crucial in mechanical design. Furthermore, its flat surfaces and well-defined edges simplify the application and interpretation of boundary conditions during both simulation and theoretical examination, thus ensuring the results are relevant to practical applications.

The selected minimum structure dimensions of 8mm x 8mm x 8mm were established to accurately assess the stress distribution without interference from the boundaries when the point load is applied to centre of the top surface. The edge effect on stress distribution with displacement between the edge and loading within 4mm is considered noticeable for the FEA. If the structure is too small, the nearby boundaries can greatly influence the stress response, complicating the isolation of the point load's impacts. By adhering to a minimum size, this study ensures that the influence of the boundaries is sufficiently captured without overshadowing the stress distributions near the point of loading, yielding more reliable and significant outcomes.

Significant features that describe the mechanical properties of the structural steel are Poisson’s ratio (μ), Young’s Modulus (E), and any pertinent material parameters. To adequately simulate the reaction of the steel structure, this knowledge is important.

The Static Structural analysis module in ANSYS was chosen for this investigation because the mechanical part is stationary and subjected to constant or slowly varying loads. Static analysis is ideal in this context, as it allows us to assess the stress distribution, deformation, and strain within the part under steady-state conditions without the influence of dynamic effects like vibrations or transient loads. For accurate simulation, hexahedral elements were employed, a robust element type in ANSYS suitable for 3D modeling of solid structures under static loading conditions. Hexahedral elements are widely used due to their capability to accurately model linear, isotropic material behavior, making them appropriate for this analysis.

Additionally, defining the structure's specific loading conditions is crucial, as these influence the behavior and response of the structure under analysis. This involves detailing any axial loads, bending moments, or other forces the structure might encounter, as well as identifying specific loading points and magnitudes. These factors directly impact the part’s stress distribution and overall structural behavior, making the Static Structural analysis with hexahedral elements an essential tool for evaluating the structural integrity and ensuring the part’s capability to withstand applied loads over its service life.

It is vital to identify the supports and restrictions that are applied to the models. These details are essential for developing a realistic simulation that accurately represents the behavior of the structural steel, regardless of whether there are fixed supports, set boundaries, or other constraints. Another important component of FEA that need consideration is meshing. To assure correct analysis investigations, it was helpful to describe the meshing method, including the kind of elements used (such as tetrahedral or hexahedral components) and the mesh density.

The kind of analysis used on the structural steel was clear and determined the extent of the study was essential for properly configuring the simulation, whether it is a static, dynamic, thermal, or a combination of these types of analyses.

Lastly, it is important to further include for any extra boundary condition, such as contact interactions or temperature conditions. These situations offer a more thorough depiction of the actual situations that structural steel could run across while it was being used.

Assuring a comprehensive and precise Finite Element study of the 12mm x 12mm x 12mm structural steel model, customised to conditions and needs of the study.

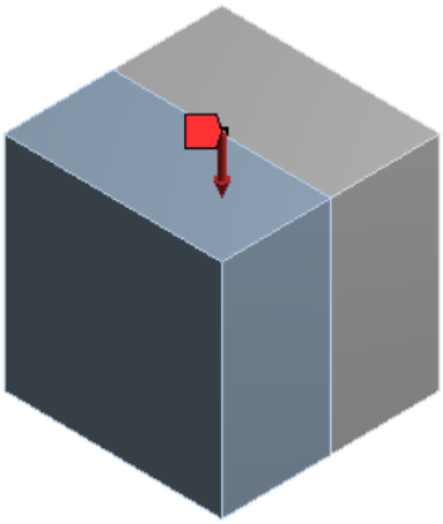

Figure 2- 2: Point load application to the structure.

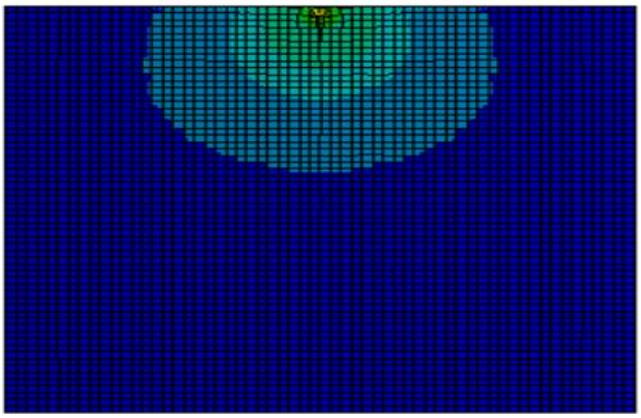

Figure 2- 3: pressure bulb formation.

Properties of Outline Row 3: Structural Steel

	A	B	C	D	E
1	Property	Value	Unit		
2	Material Field Variables	Table			
3	Density	7850	kg m^-3		
4	Isotropic Secant Coefficient of Thermal Expansion				
6	Isotropic Elasticity				
7	Derive from	Young's Modulus and Poisson's Ratio			
8	Young's Modulus	2E+11	Pa		
9	Poisson's Ratio	0.3			
10	Bulk Modulus	1.6667E+11	Pa		
11	Shear Modulus	7.6923E+10	Pa		
12	Strain-Life Parameters				
20	S-N Curve	Tabular			
24	Tensile Yield Strength	2.5E+08	Pa		
25	Compressive Yield Strength	2.5E+08	Pa		
26	Tensile Ultimate Strength	4.6E+08	Pa		
27	Compressive Ultimate Strength	0	Pa		

Figure 2- 4: Inputting the properties of the materials.

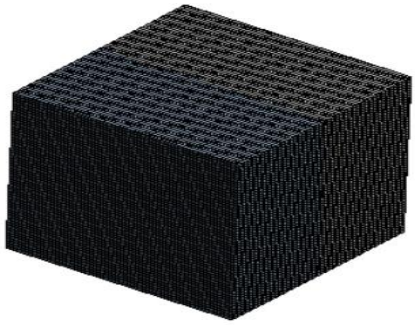

Figure 2- 5: Meshing of the mechanical structure.

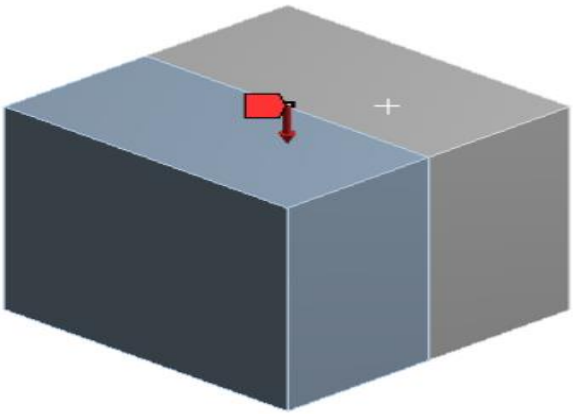

Figure 2- 6: Application of point load to the structure.

To check for mesh convergence, several simulations were done on the mechanical structure with different mesh sizes (0.2mm, 0.4mm, 0.6mm, 0.8mm, 1mm, 1.5mm and 2mm) and the results are shown below:

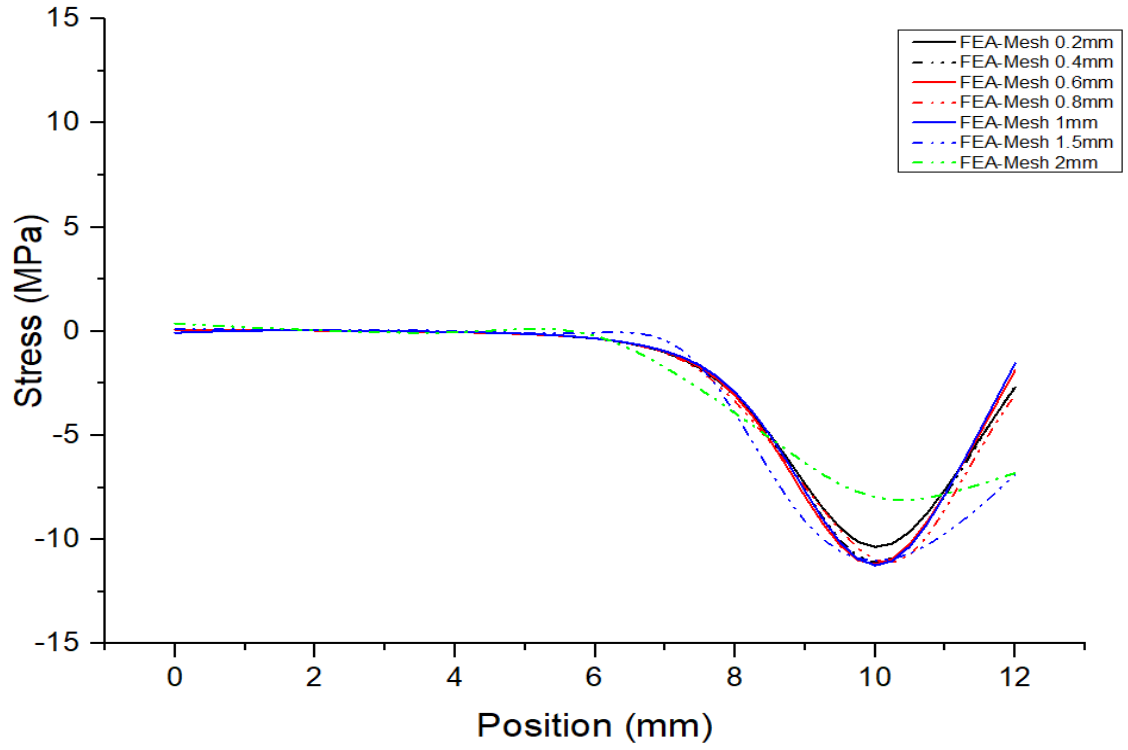

Figure 2- 7: Meshing Effect on stress distribution of the mechanical structure with limited dimension.

In Figure 2-7, the effect of mesh size on the stress distribution in a mechanical structure is demonstrated. As the mesh size decreases (finer mesh), the solution converges more closely to the true solution, resulting in a smoother and more accurate stress distribution. During the convergence study, several mesh sizes ranging from 2mm to 0.2mm were tested, with progressively smaller mesh sizes providing increasingly refined stress contours. However, it was observed that using a very fine mesh introduces practical issues, including increased computational costs and complexities in achieving convergence due to the higher number of elements.

The convergence study revealed that the mesh size of 0.2mm offered the best balance between accuracy and computational efficiency. At this size, the mesh provided a smooth and reliable stress distribution without incurring excessive computational resources or encountering significant convergence difficulties. Based on this convergence analysis, a mesh size of 0.2mm was selected for the final analysis to ensure both accuracy and efficiency.

2.1.3 Boundary and Loading Conditions

The way the structural steel model interacts with the environments and constraints was largely dependent on the boundary conditions. The boundary conditions applied to the model included a fixed support at the bottom surfaces, simulating the constraint that the structure would experience in a real-world scenario. For the side walls, a free boundary condition was chosen, allowing for lateral expansion and contraction under load. This choice was made to closely replicate the behavior of a real mechanical part where the sides are not rigidly constrained, enabling a more accurate depiction of stress distribution under realistic loading. Fixing the bottom while leaving the side walls free helps to maintain structural integrity and provides a more precise reflection of how forces interact within the material, preventing artificial stress concentrations along the edges. This boundary setup ensures that the model behaves as it would in an actual operational environment, enhancing the validity of the analysis.

The steel model's reaction to loading force may be understood by looking at the loading conditions. To investigate the behaviour of the 18mm x 18mm x 18mm model under static loading condition, a compressive force was simulated at the model's top surface by adding a vertical axial load. Important factors that vary depending on the application was subjected to the magnitude and orientation of the load.

It is vital to confirm that the boundary and loading conditions matched the real-world situation in this research work. The degree of which these situations closely resembled the real operating environment of the structural steel model determined the accuracy and pertinency the analysis results are.

2.2 FEA Results

In this section, the FEA results obtained using ANSYS software are presented. The analysis was conducted by applying a load of 100N to each of the different *LB* to observe the resulting stress distribution. For each *LB* condition, a corresponding pressure bulb was generated, visually representing the shape and extent of stress distribution within the structure. Below, the figures display the pressure distribution at each *LB,* following a logical progression to illustrate the impact of varying boundary conditions on the overall stress profile. This approach allows for a clear comparison of the pressure bulb shapes and offers insights into how boundary conditions influence stress propagation in the mechanical parts under loading.

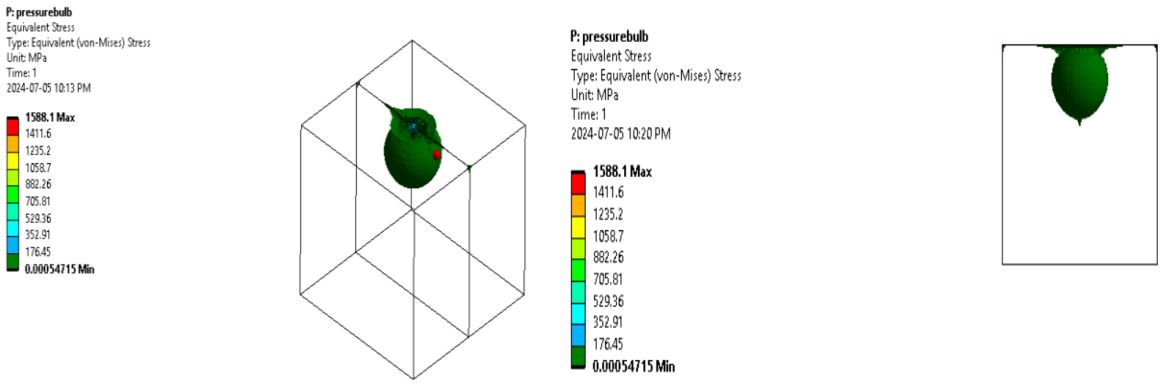

Figure 2- 8: Formation pressure bulb at 9mm *LB*.

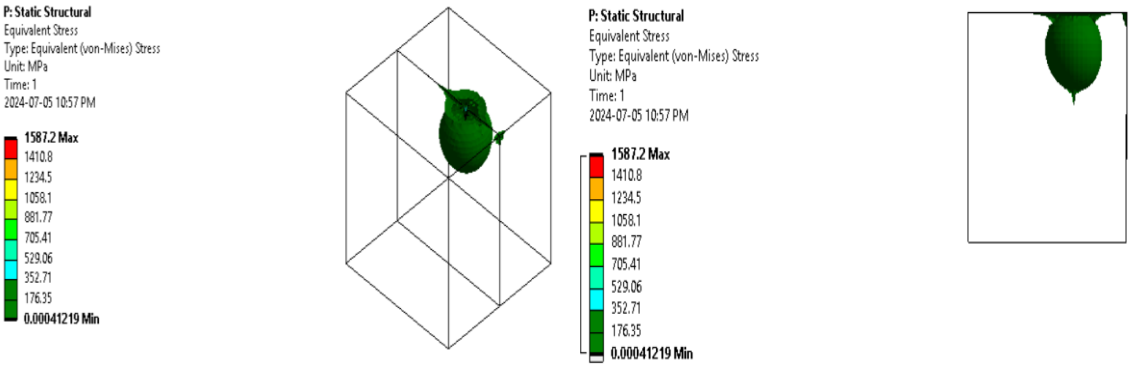

Figure 2- 9: Formation pressure bulb at 6mm *LB*.

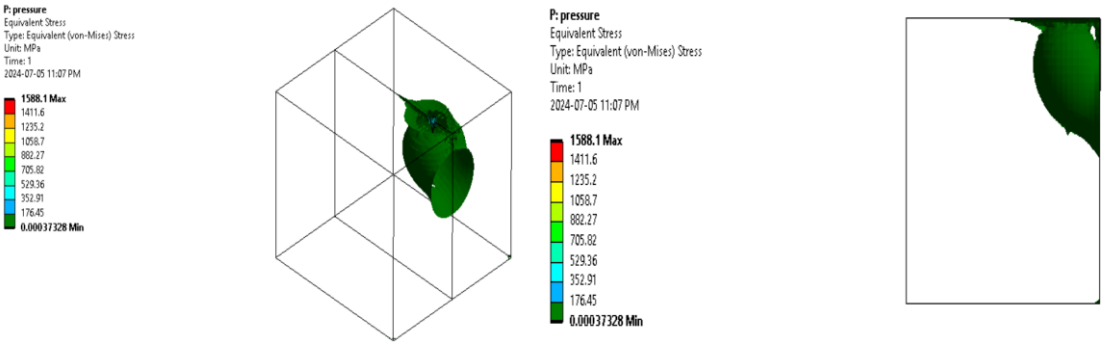

Figure 2- 10: Formation pressure bulb at 3mm *LB*.

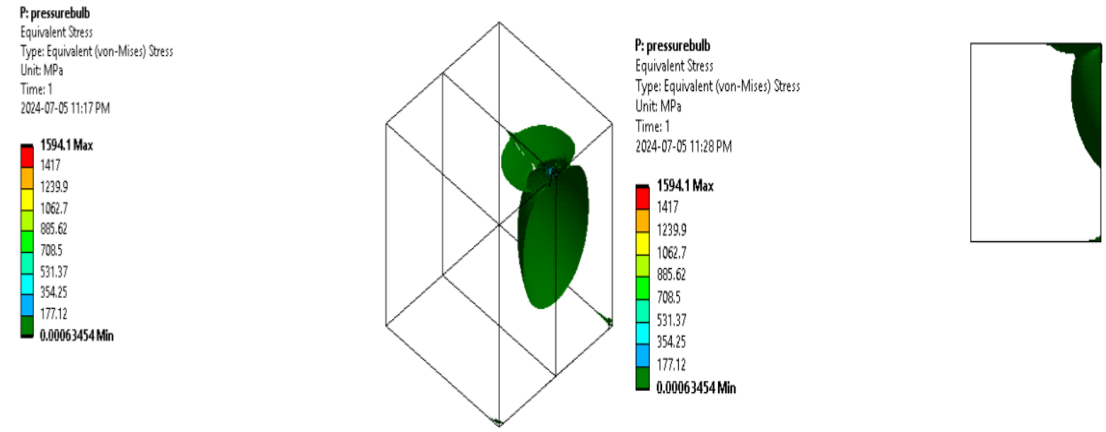

Figure 2- 11: Formation pressure bulb at 1mm *LB*.

From Figure 2-8 to Figure 2-11, the pressure bulb formation s for different *LB (9mm, 6mm, 3mm and 1mm)* show significant variations in stress distribution as depicted as shown above.

For *LB=9mm*, the pressure bulb exhibits a broad and relatively shallow distribution of equivalent stress, indicating that the stress is spread over a larger area with lower intensity. This is evident from the larger, more diffused area of high stress near the load application point and a gradual decrease in stress away from this point.

In the case of *LB*=6mm, the pressure bulb formation is more compact compared to the 9 mm case. The stress distribution is slightly more concentrated, with higher stress values closer to the load application point. This results in a smaller, but more intense pressure bulb.

When *LB*=3mm, the pressure bulb formation becomes even more concentrated. The stress distribution shows a significant peak near the load application point, with a steep gradient indicating a rapid decrease in stress away from this point. This compact pressure bulb indicates that the stress is highly localized.

For *LB=1mm*, the pressure bulb formation is the most concentrated and exhibits the highest stress values near the load application point. The equivalent stress distribution shows a very sharp peak, indicating that most of the stress is confined to a very small area. The pressure bulb is very compact and indicates a highly localized stress concentration.

Overall, as *LB* decreases from 9 mm to 1 mm, the pressure bulb becomes more compact, and the stress concentration increases significantly near the load application point. These variations in pressure bulb formations are critical for understanding how different loading conditions affect the stress distribution in the material and are essential for designing structures to withstand specific loading conditions effectively.

Chapter 3 Westergaard Model Tuning Methods and Results

In this chapter, the exploration of the processes of tuning the Westergaard model to align with FEA results was done. These includes the introduction and optimization of functions to refine the theoretical stress distribution equations. The chapter will also discuss the comparison of theoretical predictions with FEA results to validate the accuracy of the modified model.

When a point is applied to a mechanical structure, there are stress distribution and pressure bulb formed under the loaded area. To calculate the stress distribution in the structure due to one point load, the original Westergaard's equation is given as,

$$\sigma z_n(r,Z) = \frac{Q}{2\pi n^2 Z^2 (1+(\frac{r}{nZ})^2)^{3/2}}. \qquad (1)$$

$$\mathrm{n}(\mu) = \sqrt{(\frac{1-2\mu}{2-2\mu})}, \qquad (2)$$

where $\sigma z_n(r, Z)$ is the stress function at any measurement location (MPa), Q is the point load (N), μ is the equivalent Poisson's ratio, and Z (mm) and r (mm) are the depth of the measurement location and radial distance between the loading point and measurement point.

3.1 Basic Westergaard Model and Comparison with FEA

The simulation was conducted following the concept of the Pressure Bulb Theory and the FEA was done with ANSYS software. The model (18mm x 18mm x18mm) was designed with a point load at different *LB* (9mm, 6mm, 3mm and 1mm) on the horizontal. The designed mechanical structure was assigned a material property with the required Poisson ratio (Stainless Steel) and properly meshed. The Bottom part of the structure was fixed while the point load (100N) was applied. The required *"Z"* (2mm) was specified, and the function "*n*" was calculated with the required Poisson ratio. Hence, the FEA results were generated.

Where n was calculated to be 0.534522 with Poisson ratio *(μ=0.3)*. The FEA results were compared to the Westergaard Theory. The results are shown below:

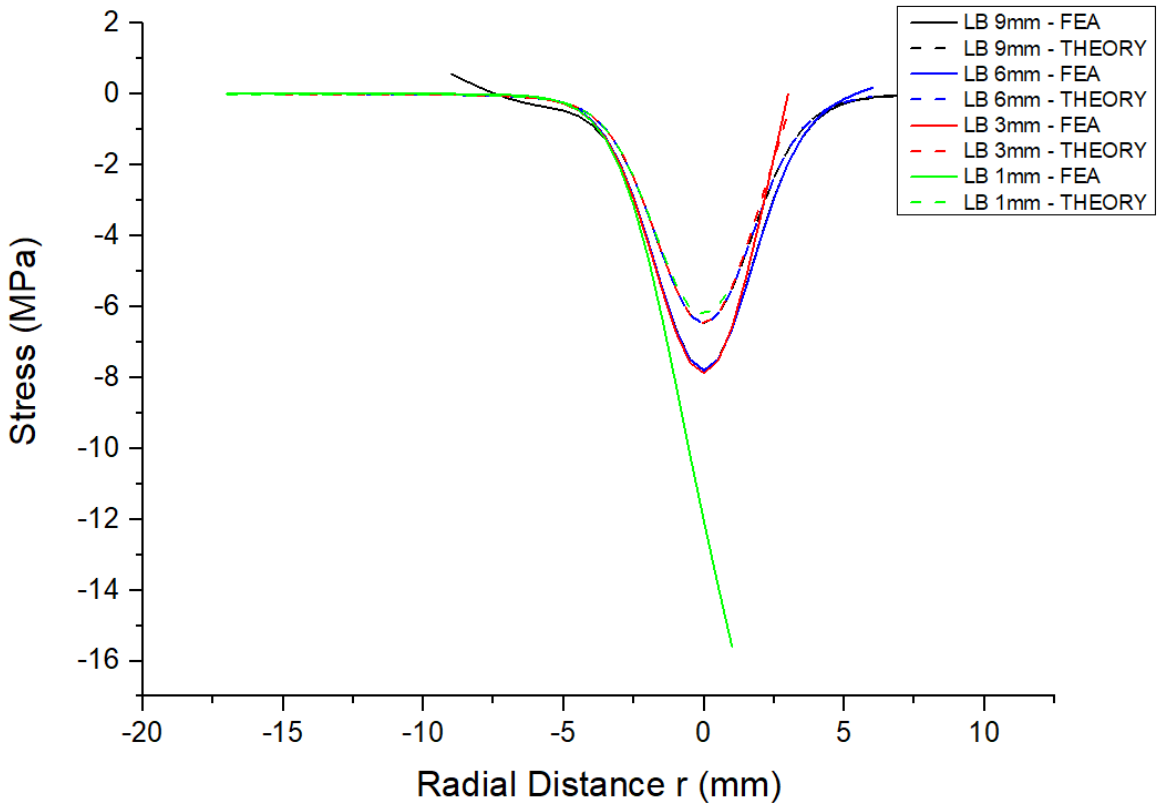

Figure 3- 1: FEA vs Westergaard at 9mm, 6mm, 3mm and 1mm LB distance.

Figures 3-1, it is shown that the Theoretical Westergaard results really differ from FEA results as shown in the curves.

To get the difference between the FEA results and theoretical results, the percentage error of the results was calculated to define the function that would make both results align. The error curves are shown below:

$$\% \, Error = \frac{FEA - THEORETICAL \, MODEL}{FEA} \times 100, \qquad (3)$$

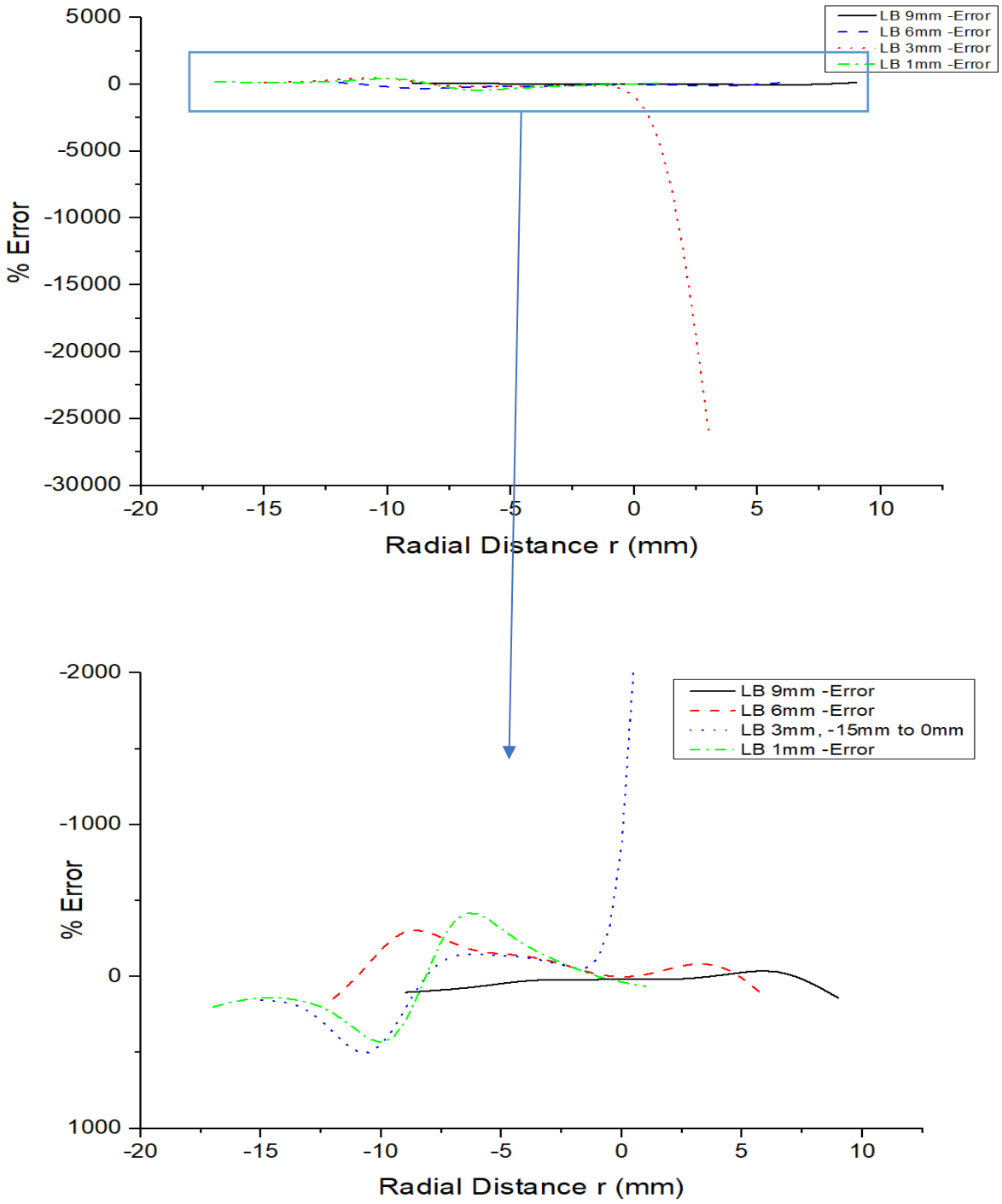

Figure 3- 2: percentage error between FEA and Westergaard at different LB (9mm, 6mm, 3mm and 1mm).

The curve in Figure 3-2 shows the percentage error between the FEA results and the Westergaard model across different loading boundaries of 9mm, 6mm, 3mm, and 1mm. Generally, the error remains low and stable across most radial distances, indicating good alignment between the two results. However, a significant error spike is observed for *LB = 3mm* near *r=0mm*, suggesting a notable discrepancy where the Westergaard model overestimates the stress compared to FEA. This highlights the need for refinement in the model, especially in regions where boundary conditions significantly affect stress distribution. The spike in the error at *LB=3mm* is shown below:

From zoomed-in data figure, the error curve presented for *LB*=3mm from -15mm to 0mm shows significant fluctuations in the percentage error across the radial distance. The positive error values near -14mm and -10mm indicate that the Westergaard model overestimate the stress compared to the FEA results in these regions. The peak error around -10mm suggests a significant divergence between the models at this radial distance. As the radial distance approaches 0mm, the error becomes negative, indicating that the Westergaard model begins to underestimate the stress compared to FEA. The sharp drop in error near -2mm suggests a sudden change in the accuracy of the theoretical model, possibly due to complex stress behavior that the model does not capture effectively. This curve highlights the limitations of the Westergaard model in predicting stress distribution accurately across different radial distances, particularly in regions with higher stress concentrations or near edges.

3.2 Methods of Modifying Westergaard Model

To align the Westergaard model more closely with the FEA results, several new functions will be introduced to modify the original equation. The goal is to improve the accuracy of stress

distribution predictions in mechanical structures by refining the existing Pressure Bulb Theory. The initially modified Westergaard equation is expressed as:

$$\sigma z_n(r, Z, LB) = K(r, LB) \times \frac{Q}{2\pi n^2 Z^2 \left(A(r) + B(r)\left(\frac{r}{nZ}\right)^2\right)^{\frac{3}{2}}}. \qquad (4)$$

Where σz_n(r, Z, LB) is the stress distribution at any measurement location *(MPa),* K(r, LB) is gaussian function introduced to account for boundary effects, *Q* is applied load *(N), r (mm)* is the radial distance from the loading point to the measurement point, *Z* is the depth of the measurement location *(mm),* A(r) is the multiplying constant function to directly influences the amplitude of the stress distribution curve around the loaded region, B(r) is also the multiplying constant function specifically to adjusts the curvature of the stress distribution function, and $n(\mu) = \sqrt{(\frac{1-2\mu}{2-2\mu})}$.

To achieve the alignment between FEA and the tuned model, the below tuning steps will be involved:

First, define and optimize A(r) and B(r) functions adjusting the shape of the Westgaard model fitting stress distribution in mechanical parts:

- Comparison between FEA and theoretical model: The stress distribution at different *r* and *Z* were calculated through the modified theoretical Westergaard model for each *LB*. Without considering the boundary effect (loading at the centre of the part), at different measurement locations, *r*, best A and B tuning parameters were found with a good match between FEA and the theoretical model.
- Rough definition of A(r) and B(r) functions: Based on the relationship between the variables, *r*, and the best tuning parameters, *A* and *B*, the functions of A(r) and B(r) were found to be an exponential function and linear function, respectively.

- Optimization of A(r) and B(r) functions: MATLAB … code was then used to further optimize the assumed functions, A(r) and B(r), by comparing with FEA results.

Second, define and optimize K (r, LB) function considering the boundary effect on stress distribution variation:

- Comparison between FEA and theoretical model: Considering the boundary effect (loading position closer to the boundary of the part), at different measurement locations, r, and load-boundary distances, *LB*, the best *K* values with a good match between FEA and the theoretical model were found.
- Rough definition of K (r, LB) function: Based on the relationship between the variables, *r* and *LB*, and the best K values, a gaussian function "K (r, LB)" was introduced to accounts for both the boundary effect.
- Optimization of K (r, LB) function: MATLAB … code was then used to further optimize the assumed functions, K (r, LB), by comparing with FEA results.

Third, consideration of the *Z* effect:

- Following the same progress defining Function A(r), B(r), and K(r, LB) functions, ZA(Z) and ZB(Z) were introduced and defined for different *Z* for no boundary effect condition, and then incorporated to the A(r) and B(r) functions, respectively, due to Z effect. ZK (Z, LB) function was also introduced to the K (r, LB) function coordinating the different boundary effects at different *Z*.

Finally, the tuned Westergaard results were calculated and compared with the FEA results for validation.

3.2.1 Introduction of Function A(r) and B(r) and the study of their effect on Stress Distribution

The Westergaard stress distribution theory's functions A(r) and B(r) are important for finding the stress distribution around a loaded point with improve accuracy. The functions in the tuned Westergaard theory are linked to the geometry and properties of material of the mechanical structure. The B(r) function relates to the curvature of the stress distribution curve, A(r) function accounts for direct influence on the amplitude of the stress distribution curve around the loaded region.

The decision to use an exponential function for defining $A(r)$ arises from the observed stress distribution behavior near the radial distance. After manually establishing $A(r)$ for each radial distance, the resulting values that closely matched both the theoretical model and the FEA results were plotted against the radial distance. The trend of these plotted values showed a close correlation with an exponential function, indicating that the stress contribution from $A(r)$ diminishes exponentially as the radial distance increases. This selection guarantees a smooth and realistic representation of stress distribution within mechanical structure under loading considering no boundary effect.

Through the incorporation of advanced material characteristics and the optimization of model functions to closely correlate with actual data, such as that from FEA, the technique exhibits a subtle adaption of a traditional structural analysis model to complex metal mechanical components. In actual engineering applications, this technique provides improved understanding and prediction of stress distributions, particularly in situations when standard models may not be sufficient.

3.2.2 Tuning of Function A(r) and B(r) with no Edge Effect

To align the FEA results with theoretical Westergaard results, tuning functions were introduced to the original Westergaard equation. Functions A(r) and B(r) were first initially assumed and introduced to the Westergaard theory to make both FEA and theoretical results be as close as possible without considering the boundary effects yet. The modified theoretical model:

$$\sigma z_n(r, Z, LB) = \frac{Q}{2\pi n^2 Z^2 (A(r) + B(r)(\frac{r}{nZ})^2)^{3/2}}. \quad (5)$$

Several assumptions were made to determine the values of the functions A(r) and B(r) as shown in equation (5) and to observe their effects on the trend of the curve. Initially, the function A(r) was varied while keeping B(r) constant at 1. Then, the process was reversed, keeping A(r) constant at 1, while varying B(r). The results of these variations are shown below:

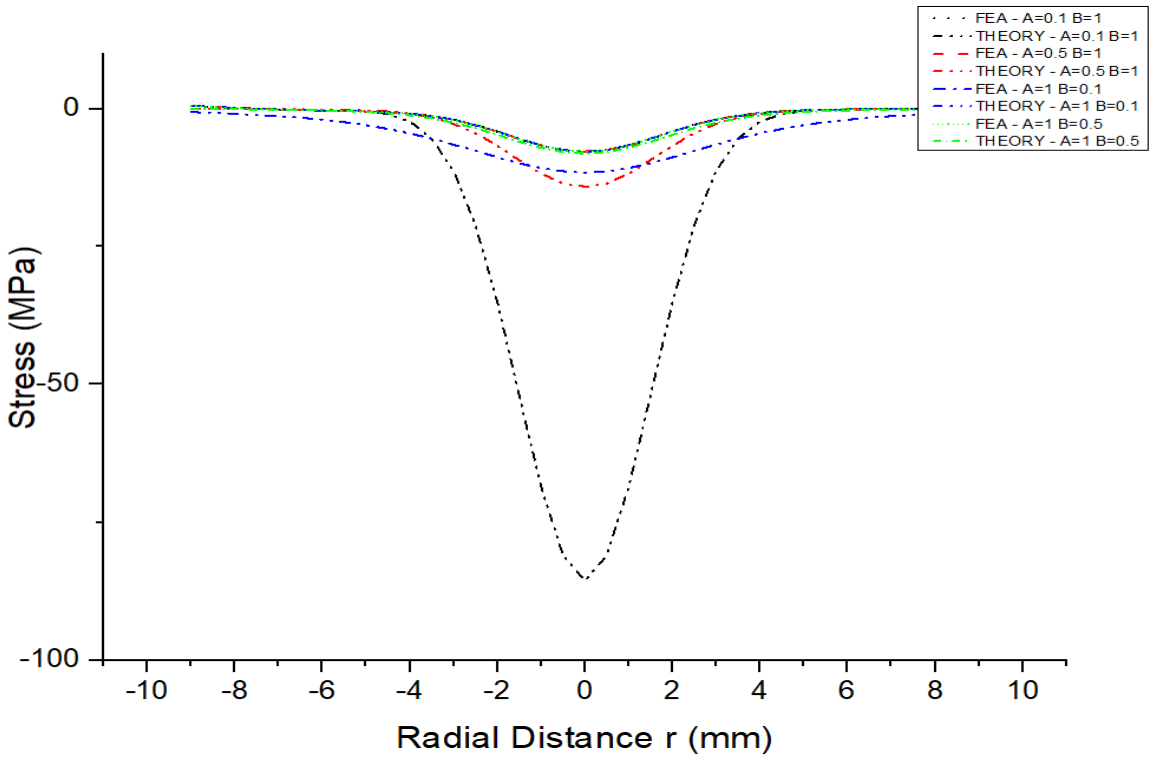

Figure 3- 3: FEA vs Westergaard Results showing the effect of A(r) and B(r) Functions.

Figure 3-3 showed that there is much difference between FEA and theoretical results. This figure demonstrates the sensitivity of the Westergaard model to the tuning of the A(r) and B(r) functions, showing that adjusting these parameters can significantly affect the predicted stress distribution. The goal is to optimize these functions to minimize the differences between theoretical and FEA results, improving the accuracy of the model for various loading conditions and material properties Top of Form Bottom of Form. The derivation of the correction function, A(r), follows these steps:

a) Manual Tuning:

Initially, the *A* value was manually tuned to match the results from the Westergaard function to those obtained from FEA at various radial distances, *r*.

b) Observation:

Upon close examination of the manually tuned *A* values at different *r*, it was observed that these values followed an exponential pattern.

c) Generalization:

To generalize the pattern and make the optimization process more straightforward, a general exponential function was formulated. The form of this function is:

$$A(r) = a \times e^{-\frac{(-(r-b))^2}{2 \times c^2}} + A_m, \qquad (6)$$

$$B(r) = 1, \qquad (7)$$

where, “a” is the amplitude or height of the Gaussian curve, “b” is the mean or centre of the Gaussian curve, “c" controls the width or standard deviation of the Gaussian curve and A_m is the amplitude and r (mm) is the radial distance between the loading point and measurement point.

The adjustment of the function A(r) makes the stress computation more align with the FEA results. The optimization technique usually applied here is probably a variation of non-linear least squares, with the aim of minimizing the discrepancy between the predictions made by the Westergaard model and the FEA results throughout the whole range of the radial distance. Considering the possible non-symmetric results from both FEA and practical cases:

a. For the two sections of the model (-9mm to 0mm and 0mm to 9mm), the parameters *a*, *b, c,* and A_m are optimised independently to take into consideration any variations in stress behaviour across the zero-point caused by loading eccentricity, material inhomogeneities, or other asymmetries. The section -9mm to 0mm and 0mm to 9mm were denoted with left (L) and right side (R) respectively in the expression below:

$$A(r) = a_{(L,R)} \times e^{-\frac{\left(-\left(r-b_{(L,R)}\right)\right)^2}{2\times c_{(L,R)}{}^2}} + A_{m(L,R)}, \qquad (8)$$

b. Because of this division, the model may be specifically fitted to each piece, resulting in a more realistic representation of the different stress characteristics of each half.

The optimization of the function *A(r)* was carried out in MATLAB by comparing the theoretical stress distribution with the simulated stress data. The optimization was performed using the "fminunc" function, which is a built-in MATLAB function for unconstrained optimization. The objective was to minimize the discrepancies between the theoretical and simulated stress values.

The initial parameters for A(r) were defined and adjusted iteratively by the optimization algorithm. The optimization process used the difference between the simulated stress data and the theoretical values computed from the modified Westergaard equation as the error metric. This error was minimized through the optimization process to achieve the best-fit values for A(r).

The function fminunc iteratively adjusted the parameters a, b, c, and A_m to reduce the sum of squared differences between the theoretical stress and FEA simulation results. The optimized parameters were then used to calculate the theoretical stress, which was compared with the simulation results for verification.

The results of the stress distribution after optimizing correction factor function, A(r), were determined. All the optimized function, A(r) parameters are tabulated below, and stresses calculated were compared with the FEA results as shown below:

Parameters	a_l	b_l	c_l	A_{ml}	a_r	b_r	c_r	A_{mr}
Values	0.90295	-0.45969	0.63984	0.10866	0.88932	0.45896	0.63304	0.12255

Table 3- 1: Values of best optimized A(r) variables with no boundary effect.

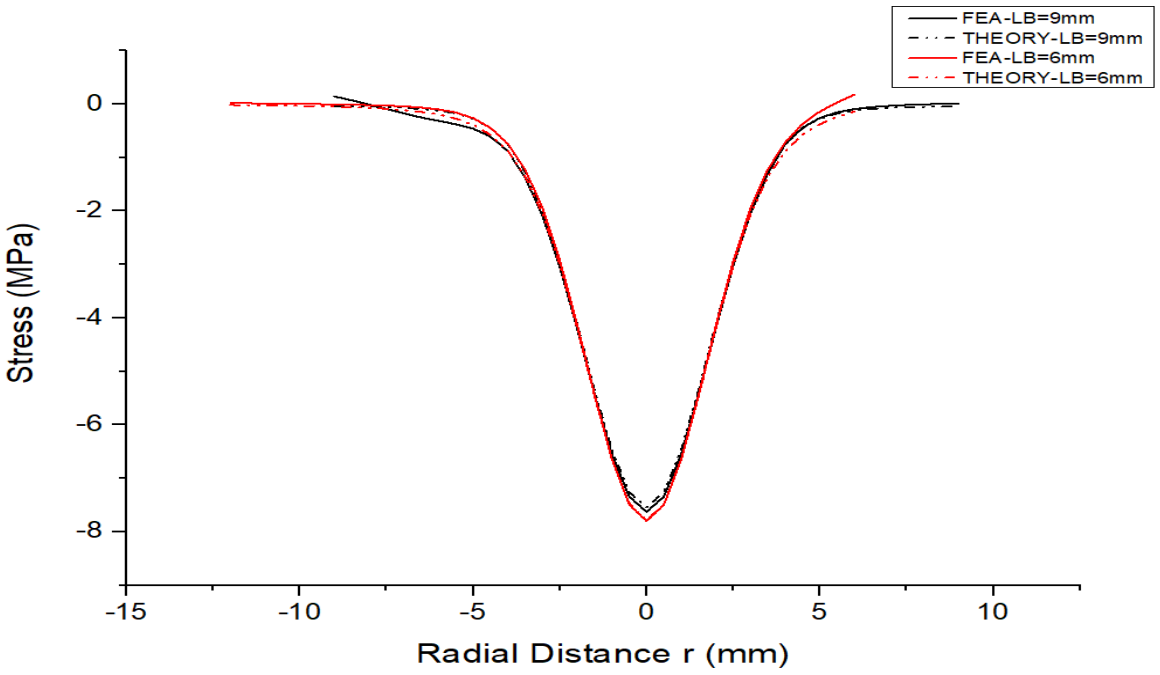

Figure 3- 4: FEA vs Westergaard equation results at different *LB* (9mm, 6mm,) at *Z*=2mm considering no boundary effect.

When tuning functions, A(r) and B(r), the absence of edge effects results in well-matched curves between theoretical predictions and FEA results when *LB*= 9mm and 6mm. This indicates that the Westergaard model, without boundary effects, provides an accurate prediction of the stress distribution at these load boundary distances. However, using the optimized A(r) and B(r) function values for when *LB*=3mm and 1mm, the result in shown in figure 3-5 below:

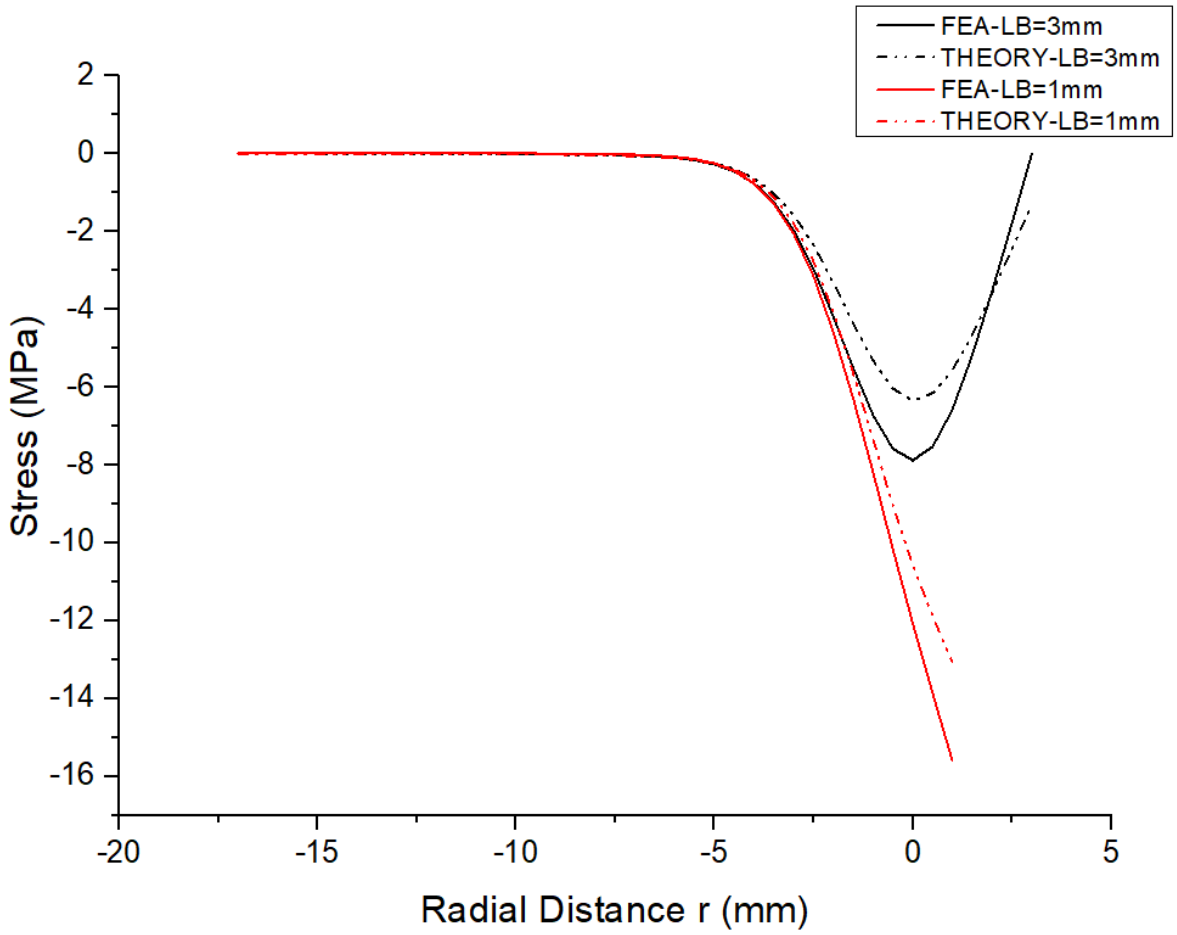

Figure 3- 5: FEA vs Westergaard equation results at different *LB* (3mm and 1mm,) at *Z*=2mm using the optimized A(r) and B(r) considering no boundary effect.

In figure 3-5, there is a more noticeable deviation between the FEA and theoretical results, and the theoretical model underestimates the stress near the boundary, indicating a need for further tuning of the Westergaard model to account for boundary effects at smaller LB values and this led to the introduction of function *K* (r, LB).

3.2.3 Introduction of Gaussian Function K (r, LB) Describing Edge Effect

In structural analysis, the "K (r, LB)" denotes the Gaussian function that affects stress distribution due to the edge effect. This function plays a vital role in understanding how stresses move through structures from their edges. Some variables including geometry, loading situation and properties of materials affects the "K (r, LB)" value. To get the K (r, LB) function, the steps taken in section 3.2.2 (manual tuning, observation, and generalization) was also adopted leading to the understanding that the edge effect can be described by a Gaussian function. The edges effect K (r, LB) function is defined below:

$$K(r, LB) = aa \times bb^{((LB-r)-3)} + cc, \qquad (9)$$

where, "aa" is the amplitude or height of the Gaussian curve, "bb" is the mean or centre of the Gaussian curve, "cc" controls the width or standard deviation of the Gaussian curve and r (mm) is the radial distance between the loading point and measurement point.

The K (r, LB) function was then optimized by adjusting its parameters, specifically *aa*, *bb*, and *cc* to achieve the best possible match between the theoretical model and FEA results at *Z*=2mm. The optimized K (r, LB) function with parameters *aa*=7.49064E-05, *bb*=0.038396923, and *cc*=0.990526363, was then applied to the model at Z=2(mm).

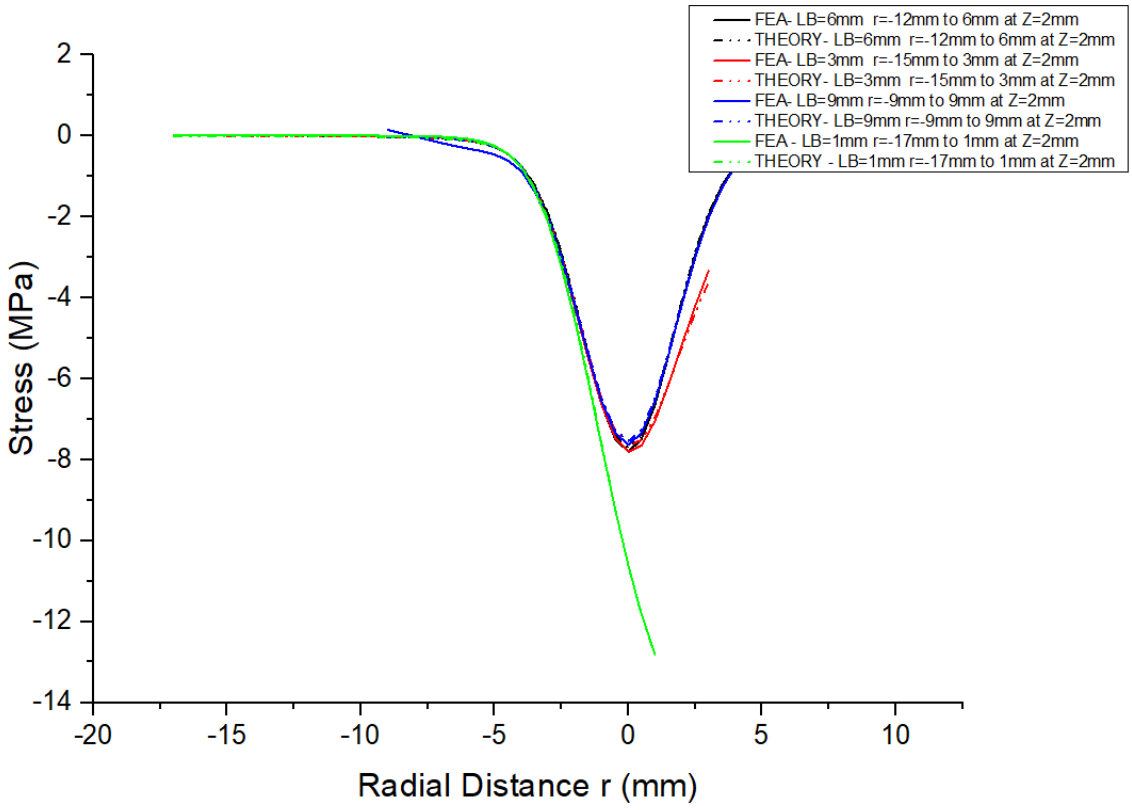

Figure 3- 6: FEA vs Tuned Westergaard using Optimized K (r, LB) function values at different *LB*=1mm, 3mm, 6mm, 9mm at *Z*=2mm.

From Figure 3-6, this tuning resulted in a good alignment between the theoretical predictions and the FEA results, demonstrating the effectiveness of the optimization process in improving the model's accuracy at *Z*=2 (mm). Next, we need to check the accuracy of the optimized K (r, LB) at different *Z*, and the results are shown in figure 3-7.

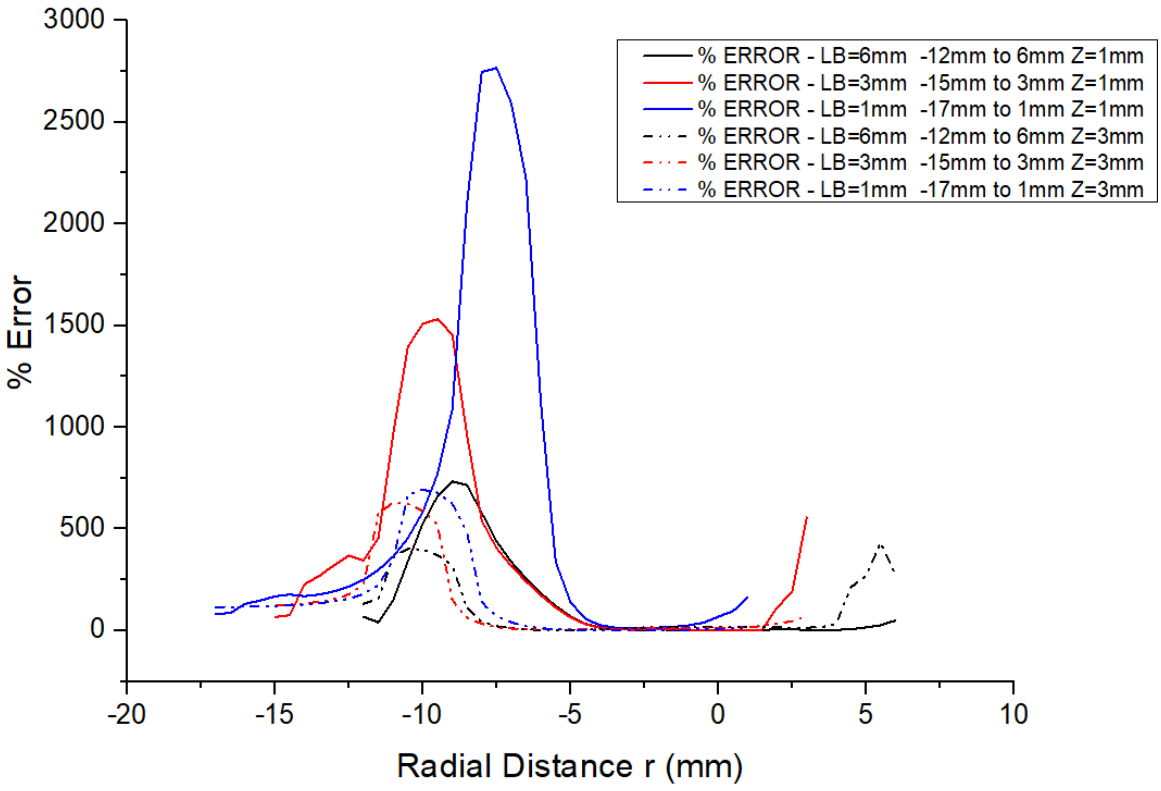

Figure 3- 7: Optimized K (r, LB) at *Z*=2mm used for evaluating the stress distribution at *Z*=1mm and 3mm.

From figure 3-7, the key observations indicate that in the high error regions, the plot reveals significant spikes in the percentage error at specific radial distances. These spikes are more pronounced when analysing the data at different *r* ranges thoroughly, particularly around *r*=−10mm to −5mm. The most substantial error is observed in the *Z*=1mm case, particularly for *LB*=1mm, indicating that the optimized parameters at *Z*=2mm do not generalize well for certain radial distances when applied to shallower depths.

The error fluctuations occur significantly across the radial distance, with some regions showing relatively low errors, indicating better alignment between the FEA and theoretical results. These fluctuations suggest that while the optimized parameters work well in some areas, they may require further tuning or adjustment for others.

The error comparison at *Z*=3mm tends to be lower overall compared to the error at *Z*=1mm. This could imply that the parameters optimized at Z=2mm are more applicable. However, the presence of considerable error spikes still indicates that the model's accuracy diminishes when moving away from the optimization *Z*.

The error curve also suggests that the boundary effects are more pronounced at certain radial distances and depths. The highest error values appear where LB is small and the boundary conditions most strongly influence the stress distribution, indicating that further refinement of the model might be necessary to better capture these effects.

3.2.5 Effect of *Z* on Tuning functions A(r), B(r) and K (r, LB)

From the discussion in the previous section, the functions ZA(Z), ZB(Z), and ZK(Z) are important in adjusting the A(r), B(r), and K (r, LB) in the context of stress distribution analysis in materials. Accurate theoretical predictions depend on these functions. The scaling function ZA(Z) has an impact on the stress distribution function's parameter A(r). Higher ZA(Z) values enhance the resistance effect, which raises the material's stress values; lower ZA(Z) values lessen this impact.

In a similar, ZB(Z) influences function B(r) while serving as a scaling factor. The shape or positional dependence of the stress distribution are frequently linked to the function B(r). The impact of geographical differences on stress is modulated by the application of function ZB(Z). While reducing ZB(Z) lessens this impact, increasing ZB(Z) increases the geometric influence on stress distribution and increases its sensitivity to positional changes.

The overall scaling of stress levels are often associated with the function K (r, LB) describing the edge effect on the stress concentration close to the structure boundary. Larger ZK (Z, LB)

values result in larger peak stresses surrounding these features because they enhance the description of the stress concentration, whereas lower ZK(Z) values result in more uniformly distributed stress throughout the material.

3.2.6 Introduction and Tuning of ZA(Z), ZB(Z) and ZK (Z, LB) Functions

The functions ZA(Z), ZB(Z) and ZK (Z, LB) were derived to fine-tune the theoretical stress distribution equations so that they align closely with results obtained from FEA at different *Z*. These functions act as scaling factors that adjust the theoretical model based on different Z and *LB*. This will lead to the finalized best A(r) B(r), and K (r, LB) functions.

The derivation of these parameters involves a combination of empirical observations and mathematical fitting to achieve the best match between theory and FEA results. The derivation of the functions followed the below sequence like the definition of A(r), B(r), and K (r, LB) functions.

I. Initial Observation and Manual Tuning

The initial step involved manually tuning the functions A(r) and B(r) by introducing the amplitude adjustment values, *ZA* and *ZB*, to match the Westgaard function to the FEA results for different *r* and *Z*. This step was critical to identify the functional form that best represents the stress distribution function considering the *Z* effect.

Z(mm)	1	1.5	2	2.5	3	3.5	4	4.5	5
ZA	1.15	1.07	1	1.02	1.05	1.1	1.15	1.2	1.25
ZB	0.65	0.8	1	1.1	1.2	1.3	1.35	1.4	1.5

Table 3- 2: Manually Optimized ZA(Z) and ZB(Z) Results

Initially random values were assumed for values of *ZA* and *ZB* (at different *Z*) at 9mm *LB* when there is no boundary effect. Based on the trend of the curves, *ZA* and *ZB* were manually optimized. The manually tuning results of the *ZA* and *ZB* functions are shown in the table above.

II. Identifying the Linear Nature

Upon manually tuning the functions at different Z, it was observed that the best fit for ZA(Z) follows a linear function. This insight led to the formation of general linear function for ZA(Z), making the model more general and easier to optimize.

III. Piecewise Linear Functions for ZA (Z), ZB(Z) and ZK (Z, LB)

To capture the variations in stress distribution for different *Z*, piecewise linear functions were employed. From Table 3-2, for any absolute value $Z < 2$mm, $ZA_1(Z)$ applies:

$$ZA_1(Z) = -0.15 \times (-Z - 1) + 1.15, \quad (10)$$

And for any absolute value of $Z > 2$mm, $ZA_2(Z)$ applies:

$$ZA_2(Z) = 0.08 \times (-Z - 2) + 1, \quad (11)$$

$$ZB(Z) = 0.08 \times (-Z - 2) + 1, \quad (12)$$

The derived ZA(Z) and ZB(Z) functions allow for accurate theoretical modelling across these ranges, demonstrating their robustness and applicability in various scenarios. The best A(r) and B(r) functions are then tuned to be:

$$Best\ A(r,Z) = ZA(Z) \times A(r) = ZA(Z) \times (a_l \times e^{-\frac{(-(r-b_l))^2}{2 \times {c_l}^2}} + A_{ml}), \text{ r<0(mm)} \quad (13)$$

$$Best\ A(r,Z) = ZA(Z) \times A(r) = ZA(Z) \times \left(a_r \times e^{-\frac{(-(r-b_r))^2}{2 \times {c_r}^2}} + A_{mr}\right), \text{ r>0(mm)} \quad (14)$$

$$Best\ B(r,Z) = ZB(Z) \times B(r) = ZB(Z) \times (r \times 0 + 1), \quad (15)$$

By following this methodology, the theoretical stress distributions closely match the FEA results, validating the derived functions and confirming their utility in predicting stress patterns in materials under different loading conditions.

As a result of discrepancies in stress distribution due to relatively smaller Z (Z < 2mm) and higher Z (Z > 2mm), ZA(Z) and ZB(Z) was introduced to make the FEA and tuned Westergaard more aligned.

Using the ZA(Z) and ZB(Z) functions as stated above for no boundary effect condition (LB=9mm), the FEA and tuned Westergaard results are shown below in figure 3-8.

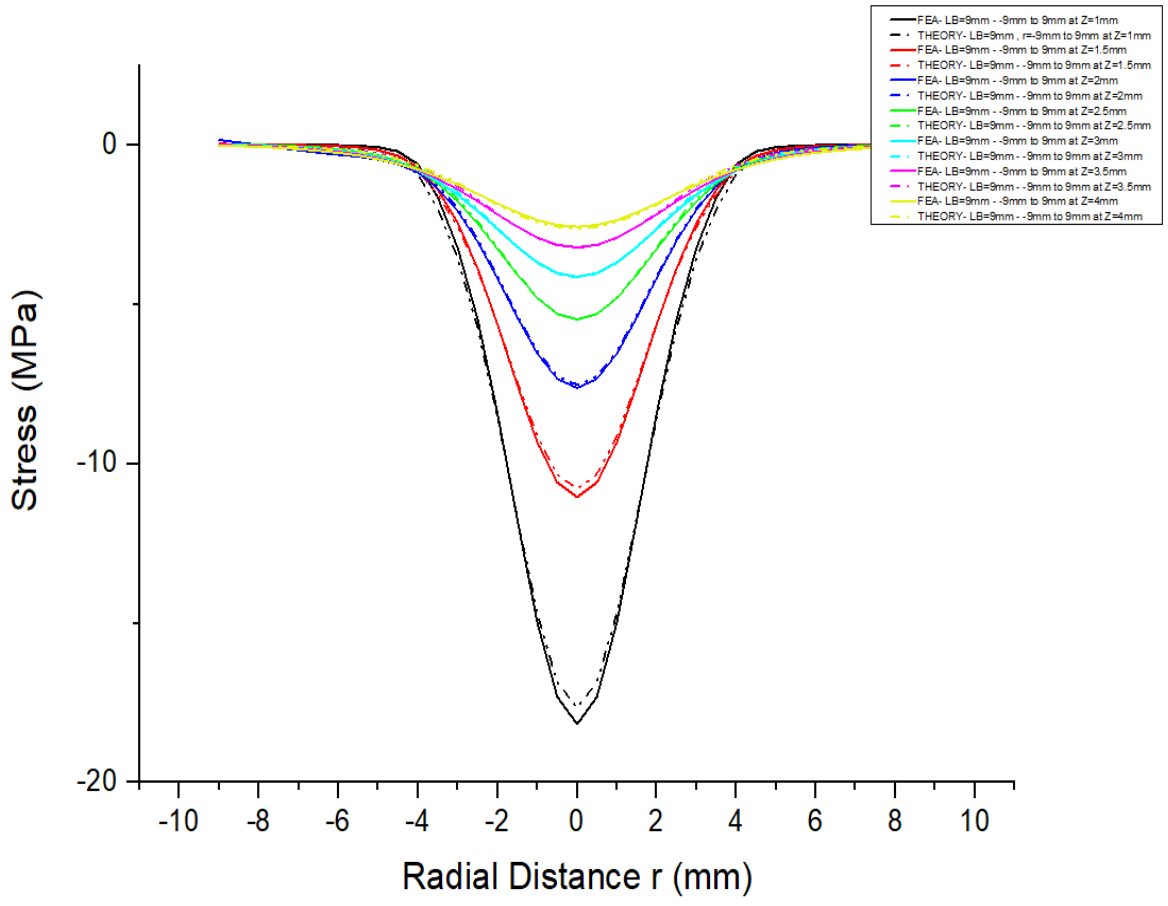

Figure 3- 8: FEA vs Tuned Westergaard for LB=9mm at different Z (Z=1mm,1.5mm,2mm,2.5mm,3mm,3.5mm and 4mm).

The K (r, LB) function plays a pivotal role in optimizing the stress distribution within the tuned Westergaard model considering the edge effects. The ZK (Z, LB) function acts as a scaling factor that adjusts the stress distribution in the tuned Westergaard model, ensuring it accurately represents the stress patterns observed in FEA. This scaling is crucial for enhancing the model's

predictive accuracy across varying depths, thereby making the tuned Westergaard model more reliable in different scenarios. The process of defining the ZK (Z, LB) function describing the depth effect on K (r, LB) follows a similar methodology used for obtaining the ZA(Z) and ZB(Z) functions. This involves a detailed optimization process of amplitude factors, *ZK*, in front of the K (r, LB) function to ensure that the model's stress distribution closely aligns with the patterns observed in FEA. Table 3-3 below shows the manually optimized values of the *ZK* values at different *Z*.

Z(mm)	1	1.5	2	2.5	3	3.5	4	4.5	5
ZK	0.8	0.9	1	1.05	1.15	1.25	1.35	1.45	1.55

Table 3- 3:Manually Optimized ZK Results.

The *ZK* values increase with *Z*, indicating that the stress concentration becomes more pronounced as the depth increases. This trend is essential for accurately modelling the stress distribution in materials subjected to varying *Z*. From table 3-3:

i. *Z* = 1mm to 2.5mm: In this range, the *ZK* values gradually increase from 0.8 to 1.05. This slight increase reflects the moderate change in stress distribution as the Z increases.
ii. *Z* = 2.5mm to 3.5mm: The *ZK* values show a more significant increase from 1.05 to 1.25. This range captures the transition where the stress distribution becomes more concentrated.
iii. *Z* = 3.5mm to 5mm: In this range, the *ZK* values continue to increase steadily from 1.25 to 1.55, indicating a higher concentration of stress distribution at greater *Z*.

The ZK (Z, LB) function's adjustment ensures that the theoretical stress calculations align closely with the FEA results across various depths. By fine-tuning the function ZK (Z, LB), the model can better account for the depth-dependent variations in stress distribution, leading to

more accurate and reliable predictions. This adjustment is crucial for applications where depth plays a significant role in stress analysis.

To account for the boundary effects after the ZA(Z) and ZB(Z) functions have been introduced, the ZK (Z, LB) function was introduced to make both FEA and tuned Westergaard results align. The ZK (Z, LB) functions was manually optimized with different *Z* and *LB*. Firstly, the *LB* was kept constant at different Z and secondly, it was observed that the slope of function ZK (Z, LB) was changing with different *LB*. The function is like an exponential function ${a_k}^{-LB}$, and the a_k was manually optimized to be 1.5.

The ZK (Z, LB) function is then introduced and derived through a process like that used for ZA (Z) and ZB(Z). The ZK (Z, LB) function was derived by closely examining the influence of *Z* and *LB* on the stress distribution in materials. An empirical approach was adopted, where a guess for ZK (Z, LB) was made based on the observed patterns. The proposed ZK (Z, LB) function is

$$ZK(Z, LB) = 1.5^{((-LB)\times 0.1875\times(-Z-2))} + 1, \tag{16}$$

And the modified best K (r, Z, LB) edge effect description function considering the depth effect can be expressed as:

$$Best\ K(r, Z, LB) = ZK(Z)\ \times\ (aa\ \times\ bb^{((\mathrm{LB}-r)-3)} + cc) = ZK(Z) \times K(r), \tag{17}$$

Till here, the theoretical stress distribution model in a part subjected to a point load considering the one single edge effect on the stress re-distribution can be obtained as below.

$$\sigma z_n(r, Z, LB) = ZK(Z, LB) \times K(r, LB) \times \frac{Q}{2\pi n^2 Z^2\left((ZA(Z)\times A(r)+(\mathrm{ZB(Z)}\times B(r))\left(\frac{r}{nZ}\right)^2\right)^{\frac{3}{2}}}. \tag{18}$$

where ZA(Z) function is defined as

$$ZA_1(Z) = -0.15 \times (-Z - 1) + 1.15, \text{Z<=2(mm)} . \quad (13)$$

And for any absolute value of Z > 2mm $ZA_2(Z)$ applies:

$$ZA_2(Z) = 0.08 \times (-Z - 2) + 1, \text{Z>2(mm)} \quad (14)$$

The formulas of depth effects on tuning function B(r) and K (r, LB) are given as below:

$$ZB(Z) = 0.08 \times (-Z - 2) + 1, \quad (15)$$

and we have

$$ZK(Z,\ LB) = 1.5^{((-LB)\times 0.1875\times(-Z-2))} + 1. \quad (16)$$

The optimized A(r), B(r), and K (r, LB) functions are summarized below,

$$A(r)_{(L)} = 0.902950477 \times\ e^{-\frac{(-(r-(-0.4595679))^2}{2\times(0.63988736)^2}} + 0.1086649, \quad (19)$$

$$A(r)_{(R)} = 0.88932428 \times\ e^{-\frac{(-(r-0.45895518)^2}{2\times(0.63304489)^2}} + 0.12254544, \text{ and} \quad (20)$$

$$K(r, LB) = 7.49064\text{E} - 05 \times 0.038396923^{((LB-r)-3)} + 0.990526363. \quad (21)$$

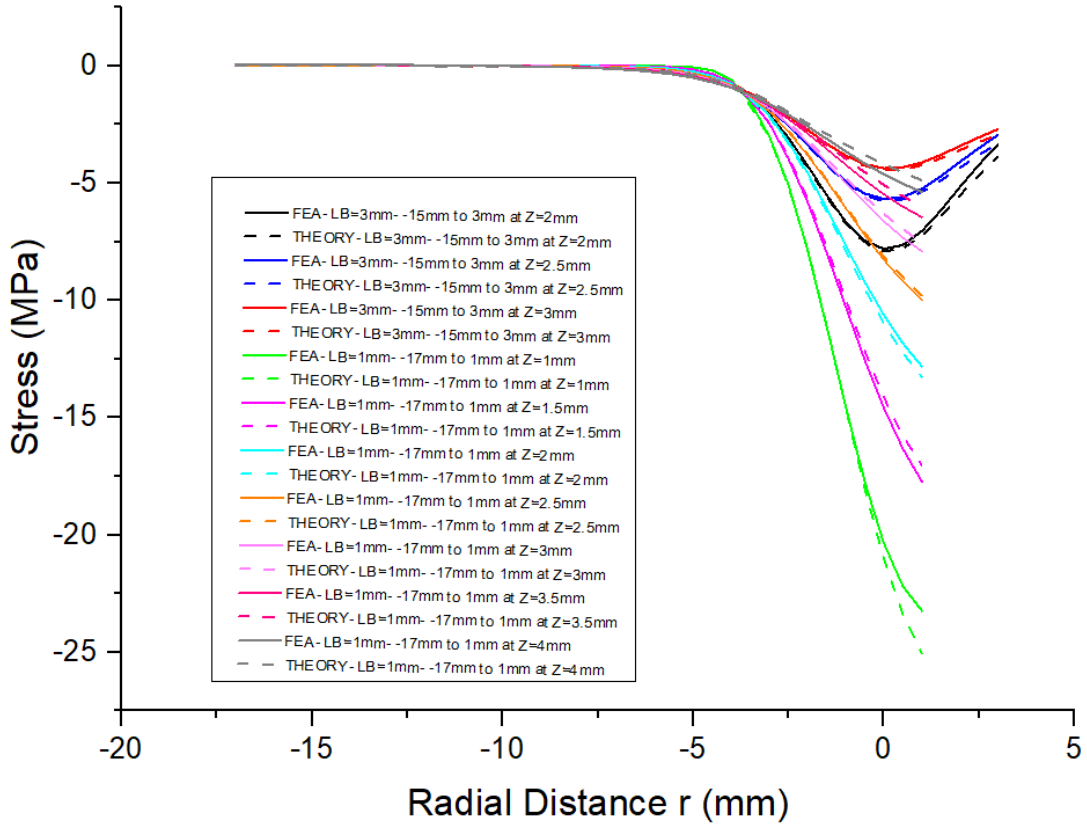

Figure 3- 9:FEA vs Tuned Westergaard for LB=3mmand 1mm at different Z

In summary, from Fig.3-9, the final tuned Westergaard formula presented above provides a robust and accurate model for predicting stress distribution in mechanical structures. The optimized functions and correction functions ZA(Z), ZB(Z), and ZK (Z, LB) are critical in ensuring the model's predictive accuracy, particularly when aligned with empirical data from FEA. This formula represents the culmination of extensive tuning and validation result, and it enhances the theoretical model's capability to predict stress patterns under various conditions. The proposed new theoretical model will be validated through some more case studies in the next chapter.

Chapter 4 Validation and Further Discussion

In this chapter, the validation of the tuned Westergaard function at different measurement locations using different structure sizes, varied point loads, and Poisson's ratios as addressed. This validation aims to double-check the accuracy and applicability of the model under diverse conditions. Additionally, the discussion of the percentage error between the FEA and the tuned Westergaard model to assess the model's reliability will also be emphasized.

To validate the tuned Westergaard function, different structure sizes (8mm x 8mm x 8mm), (12mm x 12mm x 12mm) and (20mm x 20mm x 20mm) with varied point loads, and Poisson's ratio (μ= 0.15, μ= 0.3, μ= 0.2 and μ= 0.35) were studied to show the stress distribution and alignment between FEA and the tuned model at different measurement location.

4.1 12mm x 12mm x 12mm Structure with different loads at Z=3mm

Using the tuned model, validation was done on the mechanical structure, applying different loads (150N, 250N, 50N and 200N) at a required depth. Below are the results:

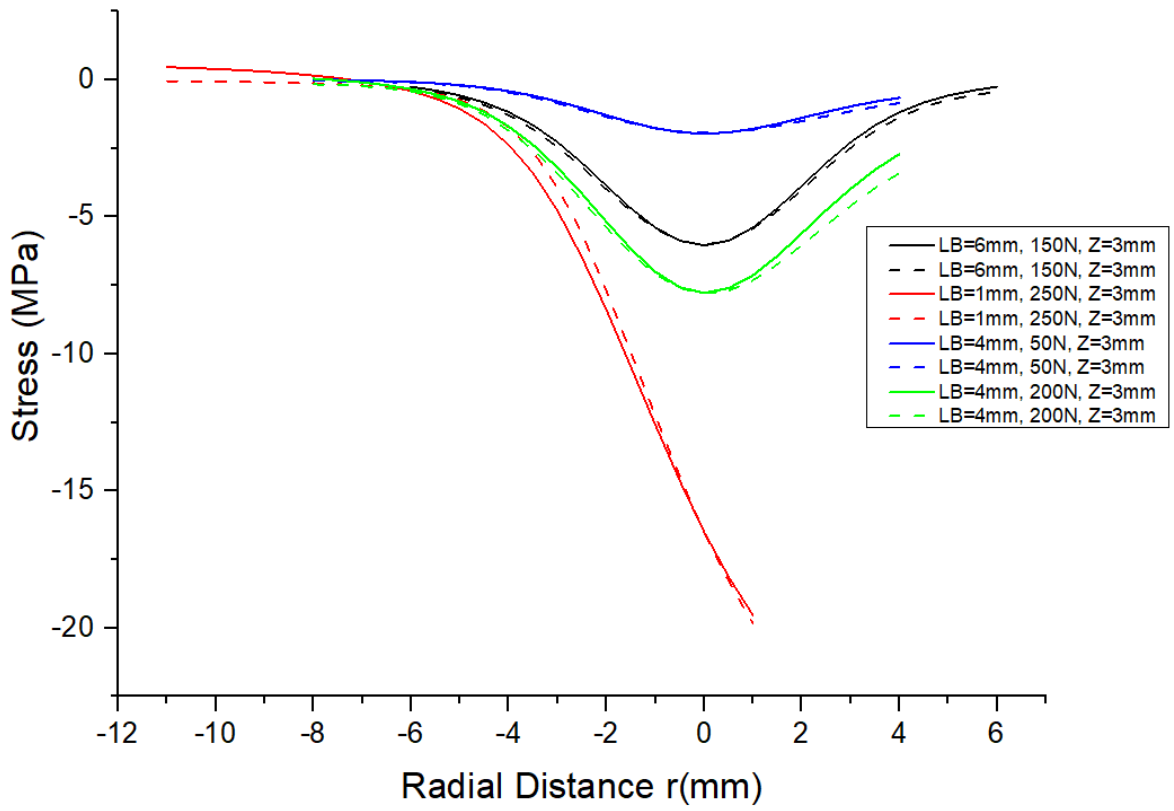

Figure 4- 1 FEA vs Westergaard equation results (for 12mm x 12mm x 12mm structure at Z=3 with point load of 150N, 250N, 50N and 200N at LB=6mm, 1mm, 4mm, and mu=0.3).

In Figure 4-1, we see the comparison between FEA results and the Westergaard theoretical predictions for a 12mm x 12mm x 12mm structure under various loads and boundary distances. The matching between the theoretical and FEA results is closer when the *LB* is larger, such as *LB*=6mm and 4mm, particularly at lower loads of 150N and 50N. The stress distribution curves for these conditions show relatively minor discrepancies, with the theoretical model successfully capturing the FEA-predicted stress trends.

As the boundary distance decreases to *LB*=1mm and the applied load increases to 200N, the mismatch between the FEA and theoretical results becomes more evident, particularly around the peak stress concentration points.

Summarizing the errors across these validation cases, it is evident that the theoretical model performs best in moderate loading conditions with larger boundary distances, where errors are minimal.

4.2 8mm x 8mm x 8mm Structure with different loads at *Z*=1.5mm

To further validate the tuned model, different *LB* and point load was used in the model at a constant *Z*. The results are shown below:

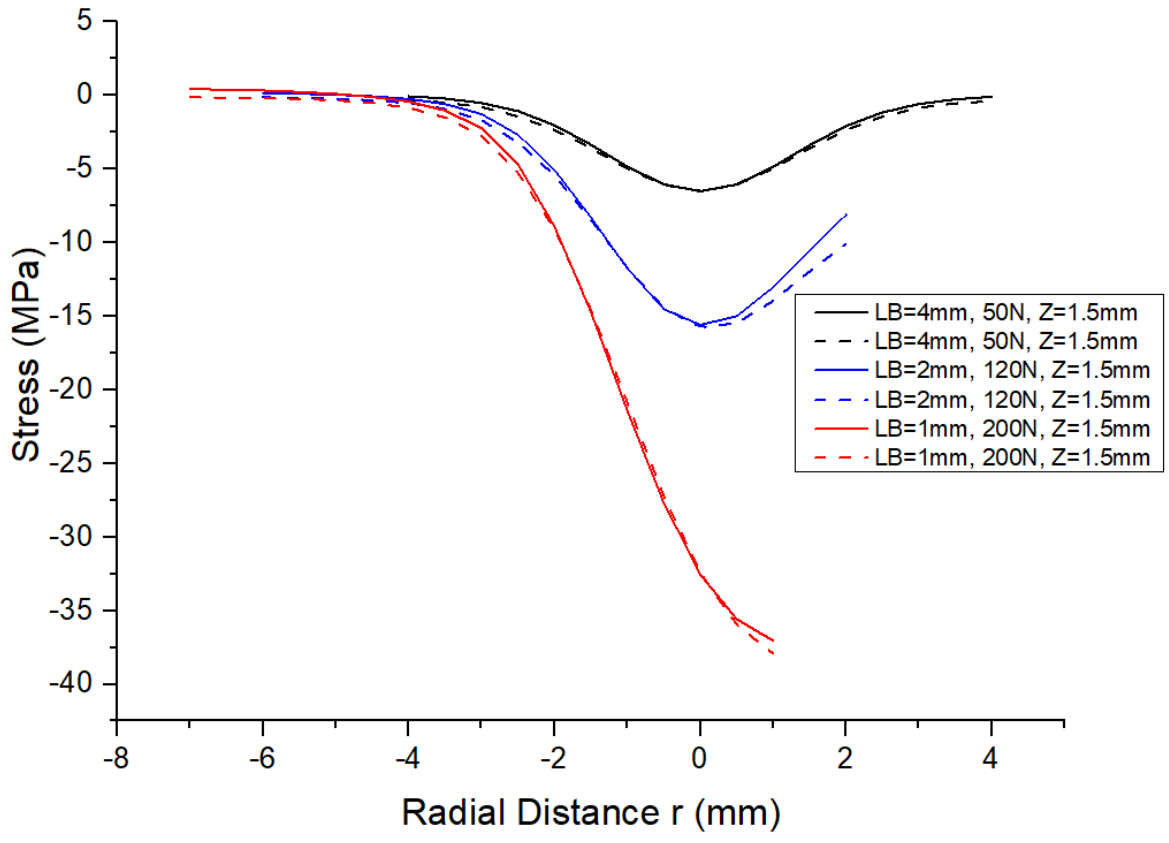

Figure 4- 2: FEA vs Westergaard equation results (for 8mm x 8mm x 8mm structure at *Z*=1.5mm with point loads of 50N, 120N and 200N and *LB*=4mm, 2mm, 1mm and mu=0.3).

The results shown in Figure 4-2 provide a comparative analysis of FEA and the tuned Westergaard equation under varying point loads and boundary distances. When analyzing the stress distribution across different radial distances, it can be observed that the FEA and theoretical results match more closely for larger boundary distances (e.g., LB=4mm) and lower loads (50N). In these cases, the error is minimal, and the theoretical predictions successfully capture the stress distribution pattern observed in the FEA results.

As the *LB* decreases to 1mm and the applied load increases to 200N, the discrepancies between the FEA and theoretical results become more pronounced. This is particularly evident in the stress concentration zones around radial distances near zero, where the theoretical model underestimates the sharp decrease in stress predicted by the FEA.

In summarizing the errors, for larger *LB* values and moderate loads, the theoretical model provides a reliable approximation of the stress distribution with relatively small errors.

4.3 Structures with different Poisson Ratios

To finally check the accuracy of the model, analysis on the tuned Westergaard was done on different structure sizes with different *Z*, *LB* and Poison's ratio. Below are the results:

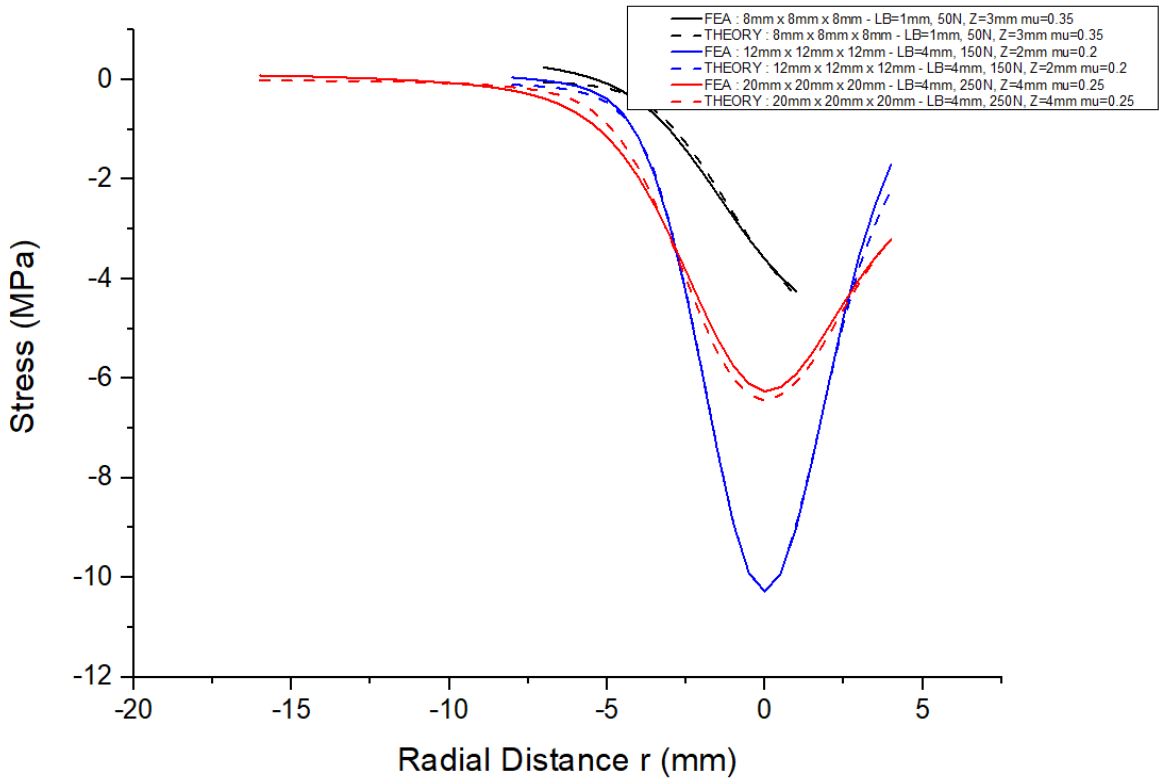

Figure 4-3: FEA vs Westergaard equation results (for 8mm x 8mm x 8mm structure with *LB*=1mm , *Z*=3mm, Load of 50N, and mu=0.35; 12mm x 12mm x 12mm structure with *LB*=4mm, *Z*=2mm, load of 150N, and mu=0.2; and 20mm x 20mm x 20mm structure with *LB*=4mm, *Z*= 4mm, load of 250N, and mu=0.25).

In Figure 4-3, the comparison between FEA results and the theoretical Westergaard model for different LB conditions, structure sizes, and material properties reveals key insights. For the 8mm x 8mm x 8mm structure with a load of 50N and boundary distance LB=1mm, the theoretical results deviate from the FEA results significantly, particularly in the regions closer to the boundary. This mismatch may be due to the inability of the theoretical model to accurately capture the effects of boundary proximity and high-stress concentration at such small boundary distances.

In contrast, for larger structures, such as the 12mm x 12mm x 12mm and 20mm x 20mm x 20mm configurations, with boundary distances of *LB*=4mm, the theoretical results closely match the FEA results, especially when the applied loads are moderate (150N and 250N). This

indicates that the Westergaard equation performs better when the boundary distance is increased, and the stress is more evenly distributed, reducing the complexity of stress concentration near the edges.

In Figures 4-1 to 4-3, the percentage errors between the FEA results and the tuned Westergaard equation were calculated using the Root Mean Square (RMS) error formula for each validation with specific part size, load, and material property. The RMS error provides an average measure of the magnitude of errors across all data points using the differences between the FEA and theoretical results, offering a clear indication of the model's overall accuracy. The error percentage of a single measurement point and its corresponding RMS calculation are given below:

$$\%Error\ (r,Z) = (\frac{FEA\ (r,Z) - \sigma z_n(r,Z)}{FEA\ (r,Z)}) \times 100, \qquad (22)$$

and the RMS error value of all measurement points within the r range of r_1~r_2 in a single case study at certain Z value can be calculated as,

$$\%\ RMSE(r,Z) = \frac{1}{r2-r1}\int_{r1}^{r2} Error(r,Z)^2 * dr. \qquad (23)$$

From the data in these figures, the RMS error values for all studied cases in our validations were found to be relatively low, with percentage errors $\leqslant$15%, indicating that the Westergaard equation provides a reasonably accurate prediction of the stress distribution. This low RMS error reinforces the reliability of the theoretical model for the general loading conditions and configurations studied.

This alignment, reflected by the low percentage errors, further validates the applicability of the tuned Westergaard model across various scenarios, showcasing its effectiveness in predicting stress distributions in the structures analysed considering a single edge effect.

Chapter 5 Conclusion and Future Works

This chapter summarizes the key findings of this thesis and discusses the improvements made to align FEA results with the tuned Pressure Bulb Theoretical results. Additionally, it will outline the potential future research directions to further refine and apply the Modified Westergaard Theory.

The primary objective of this work is to tune Pressure Bulb Theoretical results making it suitable for application in mechanical parts with limited dimension. The modified Westergaard equation represents a major improvement in the investigation of stress distribution and deformation under loaded region of a mechanical structure considering boundary effects. This advanced theory recognises the important role of the boundaries in contrast to the previous theories on mechanical structures while subjected to point load.

The most important finding is that the edge/boundary effect of a part on the stress distribution variation/concentration under a point load in the pressure bulb theory can be described by a Gaussian function. The parameters in the Gaussian function were optimized by matching with the FEA results. At the same time, additional adjustment functions of the amplitude and curvature of the traditional pressure bulb theory was introduced to the Westgaard function to enhance the accuracy of the analytical formula applied on mechanical parts made from single material.

This research work has confirmed tat this modified theory will be useful for capturing the complexities of stress distribution in mechanical structure through empirical tests, numerical approach, and real-world observations. When used with mechanical constructions, the Tuned Westergaard Theory considering the boundary effect proves to be an important resource for engineers and designers looking for a more precise approach of stress distribution and

deformation patterns. By offering insights that are more line with actual situations, this tuned model helps optimise structural design and improves the discipline of mechanical engineering.

For future studies, investigation can be done on the effects from multiple edges to analyze the stress distribution when the structure is very small or with irregular shape. For the material deformation within a linear range, we assume the multiple edge effect will be an overlay/superposition of the single edge effects that are described by Gaussian functions. But this should be further validated and studied. The multiple edge effect due to small size of some parts also has significant effect and this factor could have a major effect on the distribution of stress in a mechanical structure under study. Furthermore, the irregular shape of the mechanical structure would also be investigated to calculate the stress distribution in that kind of structure. Finally, in the future, laboratory experiment would be done on mechanical parts subjected to point loads, to further validate the tuned model with the experimental results.

Bibliography

Anderson, T. L. (2017). *Fracture Mechanics: Fundamentals and Applications* (4th ed.). CRC Press.

Bathe, K. J. (1996). *Finite Element Procedures.* Prentice Hall.

Bathe, K. J. (2006). *Finite Element Procedures.* Prentice Hall.

Bell, F. G. (1954). The Pressure of a Circular Punch on a Semi-Infinite Elastic Solid. *The Quarterly Journal of Mechanics and Applied Mathematics*, 7(3), 258-267.

Boresi, A. P., & Schmidt, R. J. (2003). *Advanced Mechanics of Materials.* John Wiley & Sons.

Boussinesq, J. V. (1885). *Application des Potentiels à l'Étude de l'Équilibre et du Mouvement des Solides Élastiques.*

Bowles, J. E. (1996). *Foundation Analysis and Design (5th ed.).* McGraw-Hill.

Brown, M. J., & O'Rourke, T. D. (2020). *Settlements and tilting of an urban building caused by tunneling. Journal of Structural Engineering.*

Burland, J. B. (1965). *The description of soil behaviour in relation to foundation design. Géotechnique.*

Burmister, D. M. (1945). *The General Theory of Stresses and Displacements in Layered Soils and Similar Materials.* Transactions, American Geophysical Union.

Chen, L., & et al. (2020). Boundary Effect Consideration in Pavement Stress Analysis: A Numerical Investigation. *International Journal of Pavement Engineering*, 21(10), 1233-1243.

Chen, Y., Yan, J., & Hu, Y. (2019). *Prediction of the settlement of a semi-floating foundation on marine deposit by the modified stress-displacement method. International Journal for Numerical and Analytical Methods in Geomechanics.*

Clough, R. W., Wilson, E. L, & Paris, P. C. (1960). Finite Element Analysis of Rigid Pavements. *Journal of the Soil Mechanics and Foundations Division*, 86(3), 1-25.

Coduto, D. P., Yeung, M. R., & Kitch, W. A. (2001). *Foundation Design: Principles and Practices (2nd ed.).* Prentice Hall.

Cook, R. D., Malkus, D. S., & Plesha, M. E. (2001). *Concepts and Applications of Finite Element Analysis.* John Wiley & Sons.

Das, B. (2010). *Principles of Geotechnical Engineering.* Cengage Learning.

Das, B. M. (2007). *Principles of Geotechnical Engineering (6th ed.).* Thomson Learning.

De Mello, V. F., & McCabe, B. A. (1992). *Determination of the state parameter of an unsaturated compacted soil. Structural Engineering International.*

Draper, N. R., & Smith, H. . (1998). *Applied Regression Analysis.*

Faisal, F. (December 2016). *Towards the Use of Piezoelectric Energy Harvesters in Pavement with Passing Vehicles.* Winnipeg: University of Manitoba.

Gazetas, G. (1991). *Soil mechanics in seismic engineering. Journal of Geotechnical Engineering.*

Gere, J. M., & Timoshenko, S. P. (1997). *Mechanics of Materials.* PWS Publishing Company.

Li, X., Ma, Z., & Wei, Z. (2022). *Evaluation of urban foundation settlement due to tunnel construction: A case study in China. Tunnelling and Underground Space Technology.*

Mesri, G. (1975). Foundation response to excavation-induced ground deformation. *Journal of Structural Engineering*, 101(1), 1-15.

Mitchell, J. K., & Soga, K. (2005). *Fundamentals of Soil Behavior (3rd ed.).* John Wiley & Sons.

Monismith, C. L., & Tapley, R. C. (1967). *Analytical and Experimental Studies of Stresses in Flexible Pavements. Transportation Research Record.*

Montgomery, D. C., & Runger, G. C. . (2010). *Applied Statistics and Probability for Engineers).*

Newmark, N. M. (1942). *Influence Charts for Computation of Vertical Displacements in Elastic Foundations.*

Ogden, R. W. (1997). *Non-Linear Elastic Deformations. Dover Publications.*

Patel, D. J., & Das, B. M. (2021). *Analytical and numerical study on the behavior of laterally loaded piles in sand under the influence of adjacent piles. Computers and Structures,.*

Potts, D. M., & Addenbrooke, T. I. (1991). The dynamic response of piled foundations: Theoretical predictions and field observations. Structural Engineering International.

Randolph, M. F., Wroth, C. P., & Farmer, I. W. (1982). Shear strength and volumetric changes in structures. Structural Engineering International.

Reddy, J. N. (2006). *An Introduction to the Finite Element Method.* (Third, Ed.) McGraw-Hill.

Roark, R. J., Young, W. C, Budynas, R. G, & Sadegh, A. M. (2002). *Roark's Formulas for Stress and Strain.* McGraw-Hill.

Sagaseta, C., Fannin, R. J, & Nicholson, P. G. (2007). *Factors influencing the measurement of the shaft resistance of piles in structures. Structural Engineering International.*

Sitar, N., & Kavazanjian, E. Jr. (2009). *Geotechnical engineering aspects of liquefaction-induced ground failures. Journal of Structural Engineering.*

Smith, J. A., & Frosch, R. J. (2010). Influence of Boundary Conditions on Stresses in Elastic Plates. *Structural Engineering Journal*, 136(7), 892-907.

Smith, J., & et al. (2018). Advancements in Pavement Analysis Using Modified Pressure Bulb Theory. *Journal of Transportation Engineering, Part B: Pavements*, 144(4), 04018040.

Smith, M. W., Reese, L. C., & Matlock, H. (2018). *Pressuremeter performance in sensitive clay. Journal of Structural Engineering.*

Terzaghi, K., & Peck, R. B. (1943). *Soil Mechanics in Engineering Practice.* John Wiley & Sons.

Timoshenko, S. P. (1953). *History of Strength of Materials: With a Brief Account of the History of Theory of Elasticity and Theory of Structures.* McGraw-Hill.

Timoshenko, S., & Goodier, J. N. (1951). *Theory of Elasticity.* McGraw-Hill.

U.S. Department of Transportation: Federal Aviation Administration. (2007). *Advanced Pavement Design: Finite Element for Rigid Pavement Joints, Report III: Model Simplification and Application.* National Technical Information Service (NTIS), Springfield, Virginia 22161.

Viggiani, G., Atkinson, J. H., & Springman, S. M. (2000). *In situ measurements of deformability properties of soil structures. Structural Engineering International.*

Westergaard, A. H. (1926). Stresses in Concrete Pavements. *Journal of the Engineering Mechanics Division*, 52(3), 1-33.

Westergaard, H. M. (1926). Bearing pressures and cracks. *Journal of the Boston Society of Civil Engineers*, 13(3), 209-214.

Westergaard, H. M. (1938). *A Problem of Elasticity in a Half-Space.* Columbia University Press.

Zhang, L., Chen, Y., & Wang, H. (2018). Incorporating Poisson's Ratio Effects in Stress Predictions. *International Journal of Structural Engineering*, 9(2), 123-140.

Zhang, Z., & Chang, M. (2015). *A probabilistic framework for considering uncertainties in the prediction of settlement of shallow foundations on granular soils. Computers and Structures.*

Zienkiewicz, O. C, & Taylor, R. L. (2000). *The Finite Element Method: Basic Formulation and Linear Problems* (Vol. 1). McGraw-Hill Education.

Zienkiewicz, O. C., & Taylor, R. L. (2005). *The Finite Element Method: Its Basis and Fundamentals.* Elsevier.